Article:
Blundell, AC, Hughes, PDM and Chambers, FM (2018) An 8000-year multi-proxy peat-based palaeoclimate record from Newfoundland: Evidence of coherent changes in bog surface wetness and ocean circulation. The Holocene, 28 (5). pp. 791-805. ISSN 0959-6836

https://doi.org/10.1177/0959683617744261

An 8000-year multi-proxy peat-based palaeoclimate record from Newfoundland: Evidence of coherent changes in bog surface wetness and ocean circulation

Blundell, A.[a*] (Corresponding author)

[a] School of Geography, University of Leeds, Leeds, Yorkshire. LS2 9JT, UK. Tel: 0113 3431593, Email: a.blundell@leeds.ac.uk

Hughes, P.D.M. [b]

[b] School of Geography, University of Southampton, Highfield, Southampton, Hants., SO17 1BJ, UK. Email: Paul.Hughes@soton.ac.uk

Chambers, F.M. [c]

[c] Centre for Environmental Change and Quaternary Research, Department of Natural and Social Sciences, University of Gloucestershire, Francis Close Hall, Swindon Road, Cheltenham GL50 4AZ, UK. Email: fchambers@glos.ac.uk

Abstract

Energy carried by warm tropical water, transported via the Atlantic Meridional Overturning Circulation (AMOC), plays a vital role in regulating the climate of regions bordering the North Atlantic Ocean. Previous phases of elevated freshwater input to areas of North Atlantic Deep Water (NADW) production in the early to mid-Holocene have been linked with slow-downs in the AMOC and changes in regional climate. Newfoundland's proximity in the North Atlantic region to the confluence of the Gulf Stream and the Labrador Current and to an area of NADW production in the Labrador Sea makes it an ideal testing ground to investigate the influence of past fluctuations in ocean circulation on terrestrial ecosystems. We use multi-proxy peat-based records from the east coast of Newfoundland to derive a proxy-climate signal for the last 8000 years, which we have compared with changes in ocean circulation. Prominent shifts towards near-surface bog water table levels, reflecting cooler/wetter climatic conditions, are evident in the early-mid Holocene *c.* 7830, 7500, 7220 and 6600 *cal.* BP with minor changes occurring *c.* 6340, and 6110 *cal.* BP. These events are coherent with evidence of meltwater injections into the N. Atlantic and of reduced NADW production. More recent increases in bog surface wetness in the mid-late Holocene *c.* 4290 and *c.* 2610 *cal.* BP are also consistent with reported periods of reduced NADW production. Coherence between the bog-derived

palaeoclimate record developed from Newfoundland and evidence of fluctuations in ocean current strength is apparent in the early mid-Holocene.

Keywords

Peatland, Newfoundland, palaeoclimate, Holocene, testate amoebae, hydrology, macrofossils

Introduction

Energy carried by warm tropical water, transported via the Atlantic Meridional Overturning Circulation (AMOC), plays a vital role in regulating the climate of areas bordering the North Atlantic Ocean (Marshall et al., 2001; Rahmstorf et al., 2015; Swingedouw, 2015). The strength of the AMOC, and in particular the production of North Atlantic Deep Water (NADW), has been found to vary through the Holocene at centennial-millennial timescales (Bianchi and McCave, 1999; Oppo et al., 2003; Hoogakker et al., 2011). Reductions in the AMOC strength are often concurrent with increased Ice Rafted Debris, evidencing freshwater export from the Arctic to Labrador and Nordic Seas (Bond et al., 2001).

Atmosphere-Ocean General Circulation modelling (Stouffer et al., 2006; Weaver et al., 2012) and ocean sediment records have demonstrated that freshwater input in to areas of NADW production in the Nordic Seas (Elmore et al., 2015) and the Labrador Sea (Carlson et al., 2008; Wagner et al., 2013) can cause potential slow-downs in the AMOC and knock-on effects to regional climate. This is typified by the so-called '8.2 ka climatic event' (Barber et al., 1999; Daley et al., 2009, 2011; Wagner et al., 2013). Meltwater released from glacial lakes, originally dammed by the Laurentide ice sheet, entered the Labrador Sea causing reduced NADW and lower temperatures in the North Atlantic area (Barber et al., 1999). Thereafter, from 7.5 to

6.4 ka, lower magnitude (>0.0015 Sv) pulsed injections of freshwater (up to 30 events) from glacial lakes in the Labrador region have been identified and noted as potentially cooling Labrador Sea Water (Jansson and Kleman, 2004).

Increased freshwater inputs to the ocean from global warming over the 20-21st century that may lead to an on-land cooling effect caused by a slow-down in the AMOC in the North Atlantic region would be nullified by the effect of the global warming trend itself Kuhlbrodt et al. (2009) suggest. However, underestimation of the sensitivity of the AMOC in models, to potential 21st century Greenland ice melt, means that this conclusion is not robust (Swingedouw, 2015). Changes in the strength of the AMOC may be critical for future climate and terrestrial environmental changes in the North Atlantic region (Rahmstorf et al., 2015). Evidence of past variability in terrestrial systems and possible influence from climate forcing mechanisms such as the AMOC are therefore crucial for the development and testing of models determining future climate projections and their influence on terrestrial ecosystems.

Newfoundland is located south of the Labrador Sea and west of the Grand Banks, a crucial junction between subtropical and sub-polar gyres of the North Atlantic where

the warm salty North Atlantic Current (NAC) and cool fresher water in the Labrador Current (LC) meet and mix (Rossby 1999; Frantantoni et al., 2010). The Labrador Sea is one of the few areas of open ocean deep convection and contributes to NADW production (Marshall and Schott, 1999). Newfoundland's eastern coast is skirted by the cold LC that exists as an inner and outer branch and transports up to two thirds of the freshwater from the Arctic Ocean (Aksenov et al., 2010), potentially influencing the strength of the NAC (Jones and Anderson, 2008) and therefore climate in Western Europe. The present-day climate of eastern Newfoundland is heavily influenced by these currents, especially the cold LC (Banfield, 1983), the inner branch of which encircles the island and is comprised of water from the Baffin and West Greenland Currents and Irminger Sea. The strength of the LC has been linked to changes in atmospheric circulation, namely the Northern Annular Mode (NAM), with positive phases associated with stronger north westerly winds, sea ice formation, cooler SSTs and iceberg transport (Drinkwater, 1996; Sicre et al., 2014). A stronger LC might be expected to reduce the influence of the Gulf Stream on the climate of Newfoundland and move its position south of Newfoundland. The location of Newfoundland in relation to these ocean currents makes it an ideal testing ground to determine the influence of past fluctuations in their behaviour on terrestrial ecosystems.

111

112 Ombrotophic peatlands offer sources of decadal to millennial-scale climate records
113 for the Holocene (Aaby, 1976; Barber, 1981; Chambers et al., 2012; Galka et al.,
114 2015; Lacourse et al., 2015; Roland et al., 2014; Blundell et al., 2016) because their
115 surface hydrological conditions react to the balance between precipitation and
116 evapotranspiration, thus reflecting climate. These climate-driven changes in bog
117 water table levels are recorded when the macrofossil remains of plant communities,
118 and associated testate amoebae microfossils from pool, lawn and hummock
119 microforms are preserved in accumulating peat. Water table shifts can be inferred by
120 reconstructing the sequence of changes in past bog surface microforms.

121

122 Although most early peatland palaeoclimate research was carried out in Northwest
123 Europe, studies are now global (Nichols and Huang 2012; Daley et al., 2012; Novenko
124 et al., 2015). However, few investigations on the North Western Atlantic seaboard
125 exist (Hughes et al., 2006; Mackay, 2016; Daley et al., 2016; Peros et al., 2016)
126 despite the widespread occurrence of near-pristine peatlands. Peatlands are
127 abundant in Newfoundland covering 18% (20,000 km^2) of the land area (Wells and
128 Pollet 1983), the oldest forming after the Newfoundland Ice Sheet retreated *c.* 9-10
129 ka (Dyke and Prest, 1987). The abundance of peatlands and its location (Figure 1)

make this area a valuable resource for exploring links between changes in ocean circulation, climate and terrestrial response. Initial work by Hughes et al. (2006) and subsequently by Daley et al. (2009) gave encouraging signs to suggest a link between terrestrial peatland ecosystems and changes in climate, regulated by changes in ocean circulation. Here we present a multi-proxy palaeo-record from Pound Cove Bog (PNDC) in Newfoundland and aim to further examine the link between past variability in terrestrial peatland ecosystems and evidence of variations in North Atlantic Ocean currents. During phases of early-mid Holocene meltwater discharges in to the Labrador Sea we aim to address the following. (1) Do palaeoecological records of water table variability in ombrotrophic bogs represent responses to changes in regional atmospheric moisture balance? (2) Are these responses coherent with the early-mid Holocene fluctuations in the AMOC variability, as seen in time series such as the IRD record (Bond et al., 2001)?

Site description

Pound Cove Bog (PNDC) is a slope bog located (Figure 1) on the western coast of Newfoundland 3 km northwest of Wesleyville on the Bonavista North Peninsula (53° 35’ 44” W 49° 9’ 59” N). The geological setting is granitic/gabbroic from the Ordovician to Carboniferous Periods and although much of Newfoundland was

covered in ice in the last glaciation, this area remained ice free (Rogerson, 1983). Slope bogs in eastern Newfoundland develop because of frequent fogs, due to the influence of the LC, and high summer precipitation levels (Damman, 1980) and, where the topography is water-shedding in all directions or where upslope snow melt is minimal, are ombrotrophic. The study site supports expansive carpets of oligotrophic Sphagna. *Sphagnum fuscum* occurs widely on hummocks, together with *Rubus chamaemorus*, *Kalmia* spp., *Chamaedaphne calyculata* and several *Cladonia* species. *Picea mariana*, *Pinus strobus* and *Larix laricina* are evident on drier bog hummocks, whilst wetter mud-bottomed hollows and pool edges are inhabited by *Rhynchospora alba* and *Eriophorum angustifolium.* *Sphagnum* section *Cuspidata* occurs in wet hollows and pools.

Field methods

A core was taken distant from expansive pools or hummocks that may prove insensitive to water table changes, in an area of deepest peat (*c.* 600 cm), from a lawn microform with extensive *Sphagnum*. Peat was recovered using a monolith tin (10 x 10 x 40 cm) from 0-40 cm and a wide-bore (9 cm) 30 cm long Russian corer (Barber, 1984) thereafter with overlaps of 5 cm. All core samples were placed in sealed plastic bags and refrigerated.

168

169 **Recovery, sampling and laboratory analyses**

170 *Recovery and sampling*

171 The core was sub-sampled for humification (2 cm^3), macrofossil (4 cm^3) and testate
172 amoebae (2 cm^3) analyses. Sampling resolution was every 4 cm for testate amoeba,
173 every cm for humification and between 2 and 8 cm for macrofossils. Sampling
174 resolution for macrofossils was variable due to time constraints; lower resolutions
175 were employed at periods of *Sphagnum fuscum* domination.

176

177 *Chronology*

178 Depths for Accelerator Mass Spectrometry (AMS) radiocarbon dating were
179 determined after multi-proxy analyses were completed. Major changes in the
180 macrofossil stratigraphy were dated using 13 AMS radiocarbon dates
181 (Supplementary information (SI) Figure 1 and Table 1)). These stratigraphic
182 boundaries represent shifts in the average position of the bog water table; however,
183 they may also indicate points at which the peat accumulation rate changed. Even
184 within *Sphagnum*-dominated peats, accumulation rates can be variable (Aaby and
185 Tauber, 1974) because of differential growth and decay rates between species
186 (Johnson and Damman, 1991). In the phase dominated by *S. fuscum* evenly spaced

187 levels were dated. Sub-sampled 1-cm³ blocks of peat were washed with deionized
188 water in a 125 µm sieve and *Sphagnum* leaves, branches or stems were selected.
189 Non-contemporaneous material was removed to prevent possible reservoir effects
190 (Kilian et al. 1995). Samples were analysed by the NERC Radiocarbon Laboratory and
191 Beta Analytic Inc. (Table 1).
192
193 An age-depth model was produced using the 'Bacon' accumulation model (Blaauw
194 and Christen, 2011) in 'R' (R Core Team, 2012). Bacon uses Bayesian statistics to
195 determine Bayesian accumulation histories using radiocarbon dates and prior
196 information. Prior information regarding peat accumulation rate and its potential to
197 vary (SI Figure 1) are accounted for in the computations, potentially providing a more
198 realistic environmentally dependent age-depth model. Bacon output provides
199 estimates for every 1 cm interval of total chronological error with maximum and
200 minimum ages within the 'modelled age range' (MAR), together with 'maximum age
201 probabilities' (MAP), to provide the most likely date. Following Turner et al. (2014)
202 and Blundell et al. (2016), dates quoted in the text are MAP and are followed by
203 MAR values in subscript, where required. All radiocarbon dates quoted unless
204 otherwise stated are calibrated.
205

206 *Proxy analyses*

207 Macrofossil analyses were carried out using the Quadrat and Leaf Count technique
208 (QLC; Barber et al., 1994), aided by a reference collection of Newfoundland bog flora
209 held at the Palaeoecological Laboratory, University of Southampton. *Sphagna* were
210 identified using Daniels and Eddy (1990) and Bastien and Garneau (1997), whereas
211 for vascular plants and non-*Sphagnum* bryophytes, Robertson (2000) and Smith
212 (2004) were employed. A Hydroclimatic Index (HCI) was calculated by weighted
213 averaging ordination (Dupont, 1986; Daley and Barber, 2012), with each taxon
214 weighted based on their relative positions along the bog water-table gradient.
215 Previous ecological observations (Wells, 1981; Wells and Pollett, 1983) were used to
216 help define weightings, *Picea mariana* = 8, Erica wood and roots = 8, Unidentified
217 organic matter = 8, Monocotyledons (undifferentiated) = 7, Dicotyledons
218 (undifferentiated) = 7, *Eriophorum spissum* = 6, *Trichophorum cespitosum* = 5,
219 *Sphagnum fuscum* = 5, *S. capillifolium* = 5, *Dicranum undulatum* = 5, *Ledum*
220 *groenlandicum* = 5, *S. magellanicum* = 4, *S. flavicomans* = 4, *S. tenellum* = 3,
221 *Rhynchospora alba* = 3, *Drepranocladus fluitans* = 3, *S. pulchrum* = 2, *S*. section
222 *Cuspidata* = 1. Small macrofossils of fruits and seeds were excluded and also
223 macrofossils with low abundance (<10% cumulatively across all levels) together with
224 shrub leaves.

225

226 Analyses to determine the humification of the peat were carried out in accordance
227 with Blackford and Chambers (1993). This involved chemical extraction of humic
228 matter, which was measured for light absorbance in a spectrophotometer at a
229 wavelength of 550 nm. Humification records can be affected by differential decay of
230 vegetation type (Caseldine et al., 2000; Yelhoff and Mauquoy, 2006; Hughes et al.,
231 2012) and may exhibit signal overwriting and temporal lags as a result of secondary
232 decomposition (Morris et al., 2015). This is partly mitigated here by producing a
233 detailed macrofossil diagram to carefully interpret results. The commonly used
234 extraction/measuring technique for peat humification has been questioned
235 (Caseldine et al., 2000; Biester et al., 2014). Biester et al. (2014) found poor
236 correlation between UV-absorption of alkali extractions and other techniques used
237 to examine peat decomposition, such as Pyrolysis GC-MS, C/N ratio, FTIR band
238 intensities and $\delta^{13}C$ and proposed that changes in the humic acids determined via UV
239 –ABS analysis of alkali extracts may reflect changes in vegetation taxa.
240

241 Samples for testate amoebae analysis were prepared and counted in accordance
242 with Charman et al. (2000). The taxonomy used here is the same as that used in the
243 transfer function applied to PNDC data and therefore taxonomic inconsistencies are

not present (Payne et al. 2010). The transfer function used was developed from North American peatlands (Booth, 2008). Counts of 100 tests are considered sufficient to be representative (Payne and Mitchell, 2009) and this was achieved for all samples. Testate amoeba records can be subject to differential preservation (Wilmhurst et al., 2003, Swindles and Roe, 2007; Mitchell et al., 2008) and some concerns exist regarding associated transfer functions employed, including spatial autocorrelation (Telford and Birks, 2009), uneven sampling of the environmental gradient (Telford and Birks, 2011) and the use of clustered datasets (Payne et al., 2012). Swindles et al. (2015) suggests that most available testate transfer functions are poor at reconstructing absolute values of mean depths to water tables but are reliable in terms of shifts in direction to wetter or drier conditions. Swindles et al. (2015) recommend reporting standardised values to avoid confusion with contemporary water-table data that report reliable magnitudes. We report absolute and standardised water-table values to aid comparison with other studies. Testate amoebae have a short life cycle and limited mobility and therefore may react to hydrological change more rapidly than plant macrofossils or humification leading to potential temporal mismatches (Väliranta et al., 2012).

262 **Results**

263

264 *Plant Macrofossils and chronology*

265 From *c*. 8070 BP $_{\text{MAR 7936-8207 BP}}$ until *c*. 6660 BP $_{\text{MAR 6534-6816 BP}}$ (PNDC a - e)

266 accumulation is relatively low at 14.9 yrs cm^{-1} as *Picea mariana, Carex*, Ericaceae and

267 *Sphagnum fuscum* are the dominant macrofossils, suggesting dry conditions (Figure

268 2). However, within this period there are two brief phases when *S. magellanicum* is

269 abundant *c.* 7830 BP $_{\text{MAR 7626-8014 BP}}$ and *c.* 7220 $_{\text{MAR 7052-7365 BP}}$, reflecting changes to

270 wetter conditions. *Drepranocladus fluitans* is abundant *c.* 6600 BP $_{\text{MAR 6472-6760 BP}}$

271 before a major shift to *Sphagnum* dominance *c.* 6500 BP $_{\text{MAR 6360-6667 BP}}$ up to the

272 surface. The switch from a system that supports *Picea* to one dominated by

273 *Sphagnum* represents a major shift in the development of the site, reflecting

274 progression to more stable water table conditions and to full ombrotrophy as taxa

275 such as *S. fuscum* (Wells and Pollett, 1983) proliferate.

276

277 From *c.* 6500 BP $_{\text{MAR 6360-6667 BP}}$ to *c.* 5530 BP $_{\text{MAR 5378-5634 BP}}$ a series of successions

278 between *Sphagnum* taxa exist with an associated increase in mean accumulation to

279 *c.* 8.3 yrs cm^{-1} . Initial succession from *S. pulcrum* to *S. magellanicum* to *S.*

280 *capilifolium* is indicative of a shift from a near-surface to a deeper water table.

Thereafter, *c.* 6340 BP MAR 6198-6497 BP *S. fuscum* peaks and is followed by increases in *R. alba, S. magellanicum* and *S. flavicomans*, representing a return to wetter conditions. Subsequent drier conditions, as evidenced by *Trichophorum cespitosum*, are succeeded by a return to *S. magellanicum* and S. *flavicomans c.* 6110 BP MAR 6004-6237 BP, the latter being dominant in zone PNDC-j and indicative of wetter conditions (Wells and Pollett, 1983).

From the mid-late Holocene, *c.* 5400 BP MAR 5216-5549 BP - 1060 BP MAR 953-1199 BP, the core is dominated by *S. fuscum*, its abundance rarely below 70% (PNDC-k – m). However, notable occurrences of other taxa include an increase in *Dicranum undulatum* (*D. bergerii*), a species that forms tufts in relatively dry conditions (Robertson, 2000), *c.* 2900 BP MAR 2657-3144 BP and peaks in *S. flavicomans c.*2460 BP MAR 2303 - 2660 BP, 1920 BP MAR 1790 - 2048 BP and 1580 BP MAR 1307 - 1837 BP, indicating increased wetness. After *c.* 1060 BP MAR 953 - 1199 BP *S. fuscum* abundance decreases as *S. pulchrum* increases *c.* 930 BP MAR 658 - 1110 BP – 630 BP MAR 372 - 899 BP suggesting a return to a near surface water table level. Post *c.* 630 BP MAR 372 - 899 BP *S. pulchrum* is succeeded by *S. magellanicum* and continued *R. alba* presence until *c.* 230 BP MAR 117 - 399 BP. Thereafter, *S. fuscum* dominates to the present day.

Sphagnum domination *c.* 6480 $_{\text{MAR 6334 - 6476 BP}}$ – 3420 BP $_{\text{MAR 3258 – 3538 BP}}$ results in a mean accumulation rate of *c.* 10.1 yrs cm^{-1}. However, a subsequent change in the bog's development to *c.* 230 BP $_{\text{MAR 117 - 399 BP}}$ leads to a decline in the mean accumulation rate to *c.* 23.4 yrs cm^{-1} despite a continued dominance of *Sphagnum*. Between 48- 24 cm (*c.* 1060 BP $_{\text{MAR 979-1170 BP}}$ – 250 BP $_{\text{MAR 128-415 BP}}$) accumulation is particularly slow at 38.6 yrs cm^{-1}. A reduced accumulation rate here may be partly explained by episodes of suboptimal conditions for peat accumulation, such as the development of a pool as evidenced by *S. pulchrum* and *R. alba* in Zone PNDC-n. Taxa associated with pools have been recorded as exhibiting high rates of decay (Johnsen and Damman, 1991; Belyea, 1996; Limpens and Berendse, 2003). From *c.* 630 BP $_{\text{MAR 372-899 BP}}$ (36 cm) *S. magellanicum* and subsequently *S. fuscum* dominate to the surface.

Humification

Periods dominated by *Sphagnum* display low levels of decay, whereas assemblages containing more degradable plant matter, with a lower nitrogen concentrations (Coulson and Butterfield, 1978), such as monocotyledon or Ericaceae remains, register higher levels of humification. Phases are apparent in the record where complex fluctuations occur around a broadly stationary average humification value

(Figure 3). For example, Zones PNDC a-e, containing *Picea*, monocots and UOM remains, show high residual absorbance values compared with zones f-h, which are lower as *Sphagnum* moss becomes abundant. From PNDC-i to midway into PNDC-k a lower average absorbance residual is evident, again commensurate with greater abundance of *Sphagnum*. From 250 cm depth to the start of PNDC-l, average absorbance residuals increase and further increase in PNDC l-m. Major fluctuations in humification in these zones are often associated with increases in monocotyledon and Ericaceae remains that have a disproportionate effect on humification values, representing evidence of 'species-dependent effects' (Yeloff and Mauquoy, 2006). Major changes to low absorbance that cannot be accounted for by shifts in the colouration of the contributing plants and potentially reflect water table variability caused by climate change are shown in Supplementary Information (SI) Table 1.

Testate amoebae

Dry-indicating testate amoebae including *Hyalsophenia subflava*, *Nebela militaris/minor* and *Trigonopyxis arcula* (Booth, 2008) are prevalent (Figure 4) in Zones PNDC-a – PNDC-e (*c.* 8020 BP $_{\text{MAR 7865-8163 BP}}$ – 6600 BP $_{\text{MAR 6472-6759 BP}}$). However, increases in hygrophilous taxa *Archerella flavum* occur, leading to relatively wetter conditions and lower reconstructed depth to water tables (DTWTs) *c.* 7830 BP $_{\text{MAR}}$

7626-8014 BP, *c.* 7500 BP MAR 7336 – 7694 BP, and *c.* 7220 BP MAR 7053-7366 BP. PNDC-e is dominated by *N. militaris/minor* reflecting drier conditions (Amesbury et al., 2013). This supersedes a substantial change to wetter conditions as both *Archerella flavum* and *Amphitrema wrightianum* increase *c.* 6600 MAR 6472-6759 BP, the latter peaking *c.* 6480 BP MAR 6334-6643 BP. Further switches from *N. militaris/minor* and *H. subflava* to the hygrophilous *Archerella flavum* and *Amphitrema wrightianum*, occur at the lower boundary of PNDC-h *c.* 6340 MAR 6198-6497 BP, and 6110 MAR 6004-6237 BP. PNDC-I and PNDC-j are dominated by *Archerella flavum* and only *c.* 5370 BP MAR 5183 -5531 BP do more xeric taxa such as *N. militaris/minor* and *T. arcula* return. In PNDC-k four substantial increases in *Archerella flavum* occur *c.* 5010 MAR 4815 -5198 BP, 4500 MAR 4311 - 4669 BP, 4290 MAR 4117-4477 BP, 4010 MAR 3889 -4145 BP and 2950 MAR 2680 -3187 BP and these events are associated with declines in the xeric taxa *H. subflava*, *N. militaris/minor*, *T. arcula* and *Difflugia pulex,* suggesting changes to wetter conditions. Increases in *Archerella flavum* and *Amphitrema wrightianum* are also evident in PNDC-l *c.* 2610 BP MAR 2428-2830 BP and *c.* 2110 BP MAR 1974-2319 BP.These changes are followed by elevated levels of the xeric *H. subflava,* commencing *c.* 1920 MAR 1790 -2048 BP. Subsequent increases in *Archerella flavum*, and *Amphitrema wrightianum* and decline in *N. militaris/minor* and *T. arcula* are evident *c.* 1480 MAR 1219-1755 BP, 1250 MAR 1060 -1490 BP and *c.* 290 MAR 161 -467 BP, indicating a return to wetter conditions. Substantial changes

357 to wetter conditions (from high reconstructed DTWTs to low values) are displayed in
358 SI Table 1.
359
360 **Discussion**
361 *Comparisons of proxy palaeoclimate signals*
362 Proxy techniques used in this study for palaeo-hydrological reconstruction require
363 careful cross-examination since 'palaeoclimate' signals derived can be influenced by
364 other non-climatic factors (Blundell and Barber, 2005; Swindles et al., 2012).
365 Reconstruction of bog surface wetness (BSW) should be informed by all available
366 sources of evidence where possible (Blundell and Barber, 2005). Changes to wetter
367 conditions evident in each proxy and when at least two of the three proxies are in
368 agreement (Figure 5) is stated in SI Table 1.
369
370 Standardised values for outputs from three testate amoebae transfer functions,
371 humification and macrofossil HCI are compared to highlight similarities and
372 differences between the palaeoclimate proxies at PNDC (SI Figure 2). Transfer
373 functions from Booth (2008) and Amesbury et al. (2013) show good correspondence
374 ($r^2 = 0.696$, $p < 0.0001$), but data from using the Charman and Warner (1997)
375 function do not show good correspondence with the other two functions of Booth

376 (2008) (r^2 = 0.058, p = 0.004) and Amesbury et al. (2013) (r^2 = 0.180, p < 0.0001). At
377 Nordan's Pond Bog (Newfoundland) Hughes et al. (2006) used the Newfoundland-
378 specific transfer function (Charman and Warner, 1997) to reconstruct water table
379 depth; however, its use highlighted concerns related to the representation of specific
380 taxa such as *Hyalosphenia papilio*, and *H. elegans*. In the training set these were
381 modelled (Charman and Warner, 1997) as having relatively high DTWT optima, and
382 resultant DTWT reconstructions displayed 'conflicts' with the other proxies. Optima
383 were substantially higher than those subsequently derived from other European
384 (Charman et al., 2006; Amesbury et al., 2016), British (Woodland et al., 1998), North
385 American (Booth, 2008) and north-eastern Canada and Maine (Amesbury et al.,
386 2013) based functions. This, in part, led to the poor correlations with the other proxy
387 indicators (humification r^2 = 0.007, p = 0.321; HCI r^2 = 0.03, p = 0.041) and therefore
388 the Charman and Warner function is not employed.
389
390 The macrofossil HCI data exhibit low variability (SI Figure 2a-d) owing to the
391 dominance of *S. fuscum*. Variability that is present is concentrated at the high (dry)
392 and low (wet) extremes and it is broadly in agreement with the extremes of both
393 humification and testate amoebae derived BSW data (SI Figure 2 and SI Table 2). The
394 highest HCI correlation (SI Table 2) is with the testate amoebae transfer function

395 from Booth (2008) (r^2 = 0.401, p < 0.0001). Even when the record is dominated by
396 *Sphagnum fuscum,* peat humification values vary considerably, suggesting that these
397 are not species-dependent changes but more likely reflect changes in bog water
398 table. Some peaks in humification are concurrent with small amounts of low-C/N
399 plant material (Coulson and Butterfield, 1978), which can deliver a disproportionate
400 contribution to the peat decay signal (Yeloff and Mauquoy, 2006) owing to their ease
401 of decomposition. The early macrofossil record before *c.* 5400 BP MAR 5216-5549 BP,
402 which is not dominated by *S. fuscum*, is in close agreement with both testate and
403 humification signals. Thereafter, the macrofossil record is hydrologically insensitive.
404
405 The humification record, once reduced to 4 cm resolution by removing values to
406 align it with that of the testate amoebae DTWT reconstruction, displays the closest
407 correspondence (r^2 = 0.257, p = <0.0001) with the DTWT reconstruction based on the
408 Booth (2008) transfer function, followed by that from Amesbury et al. (2013) (r^2 =
409 0.143, p < 0.0001) and a poor correspondence with the function devised by Charman
410 and Warner (1997). The testate transfer functions from Booth (2008) and Amesbury
411 et al. (2013) give similar outputs but the former displayed most correspondence with
412 other proxies and is therefore used here.
413

414 Particular differences between the humification record and the DTWT reconstructed
415 from testate amoebae (derived from Booth, 2008) are evident *c.* 1060 BP $_{\text{MAR 953-1199 BP}}$
416 – 1190 BP $_{\text{MAR 1039-1378 BP}}$, *c.* 2330 BP $_{\text{MAR 2128-2562 BP}}$, *c.* 2910 BP $_{\text{MAR 2657-3145 BP}}$, *c.* 3880
417 BP $_{\text{MAR 3721-4029 BP}}$, *c.* 3950 BP $_{\text{MAR 3817-4089 BP}}$, *c.* 4150 BP $_{\text{MAR 3997-4317 BP}}$ and require
418 interpretation. In these instances humification values are relatively high, whereas
419 reconstructed DTWTs from testate amoebae data are relatively low (high water
420 table). Examination of the macrofossil record reveals that these are periods of pool
421 mud deposition or there is evidence of a small percentage of more degradable
422 material such as *Rhynchospora alba*, both of which are indicative of wet conditions.
423 From *c.* 4890 $_{\text{MAR 4713-5063 BP}}$ – 5280 $_{\text{MAR 5073-5458 BP}}$ BP and *c.* 7860 BP $_{\text{MAR 7653-8037 BP}}$ the
424 converse applies as *Sphagnum* dominates but high percentages of the testates *H.*
425 *subflava* and *T. arcula* point to a low water table. A potential lag between
426 humification and DTWT reconstructed from testate amoebae is evident *c.* 2980 BP
427 $_{\text{MAR 2720-3212 BP}}$ and *c.* 4520 BP $_{\text{MAR 4329-4684 BP}}$, as the latter appears to react a sample
428 before the humification record. Changes to wetter conditions evident in each proxy
429 and when at least two of the three proxies are in agreement (Figure 5) is stated in SI
430 Table 1.
431

In the last few decades, changes in vegetation, reconstructed DTWTs, and humification have largely been interpreted as the result of allogenic factors, predominantly changing climate. However, anthropogenic disturbances can affect the bog hydrological conditions, through burning, artificial drainage, peat cutting and atmospheric pollution. The role of autogenic factors has been revisited (Swindles et al., 2012; Morris et al., 2015; Waddington et al., 2015) and highlighted through the differences displayed between multiple cores from the same site (Blaauw and Mauquoy, 2012; Mathijssen et al., 2016), suggesting that internal 'noise' exists within the fossil proxy records together with a climate signal. Infilling of pools and increasing DTWTs can, for example, occur as a result of peat accumulation under stable climate conditions (Aaby, 1976). Although peatland water table levels are sensitive to climate change, the peatland archive can be affected by non-linear complex internal responses (Swindles et al., 2012). Determining climate signals can be achieved by examining multiple cores at a site or from adjacent sites, although this approach is costly and not always practical. However, similarities between other well-dated records can provide increased confidence that changes in peat stratigraphy are externally driven.

Comparison of PNDC with Nordans Pond Bog (NDN)

451 The peat-based palaeoclimate record at NDN (Hughes et al., 2006) is located within
452 two kilometres of PNDC. Coherent changes should reflect climate as opposed to
453 autogenic influences. Since publication (Hughes et al., 2006) the age–depth model
454 has evolved (Daley et al., 2009; 2011) and tephra layers have been discovered (Pyne-
455 O'Donnell et al., 2012) at NDN providing additional dating. Five of the tephras found
456 have a reliable date assigned to them and have been used here to improve the
457 original age–depth model (SI Figure 3). To permit comparison with PNDC, testate
458 amoebae-derived DTWTs from NDN have been recalculated using the transfer
459 function of Booth (2008). Here we have compared the two testate amoebae records,
460 as these are the most robust of the three proxies; the macrofossil record post *c.*
461 5400 BP $_{\text{MAR 5216-5549 BP}}$ at PNDC is hydrologically insensitive and the humification data
462 can be affected by site specific changes in vegetation requiring more protracted
463 consideration. Differences in sampling resolution, allied with potential chronological
464 error, make comparison challenging. However, from the early Holocene to *c.* 4000 BP
465 nine of the 10 most prominent changes in the PNDC testate amoebae record can be
466 associated with similar events at NDN, well within dating errors (Figure 6 and SI
467 Table 1). Thereafter, although variation in the NDN record is relatively low some
468 prominent changes to wetter conditions at PNDC can be linked to changes at NDN
469 within dating errors. The substantial change at PNDC *c.* 1480 BP $_{\text{MAR 1219-1755 BP}}$ is just

within dating errors of a similar change at NDN (*c.* 1780 BP MAR 1646-1905 BP), but matching these is less robust. Although there are similarities in hydrological changes between the two study sites suggesting a climate-forcing mechanism was acting on these two adjacent but hydrologically-separated peatland systems, the chronological control is insufficient to conclude definitively.

The palaeoenvironmental record at PNDC and comparisons with proxies of ocean circulation and terrestrial paleoclimate records.

Mid Holocene (8000 – 5000 BP) The PNDC record displays a series of prominent increases in bog water table levels to wetter conditions in the mid-Holocene *c.* 7830 BP MAR 7626-8014 BP and 7500 BP MAR 7336 – 7694 BP, followed by further episodes *c.* 7050 MAR 6847-7247 BP and 6480 MAR 6341-6653 BP. Comparisons with wider oceanographic evidence from the eastern seaboard region, discussed below, suggest that these changes in BSW on the Bonavista North Peninsula are most likely the result of reduced evapotranspiration from cooler climatic conditions (Figure 5 and 7) and/or elevated levels of precipitation. Evidence presented by Jansson and Kleman (2004) suggests that the eighth millennium BP was a period of heightened sensitivity of the AMOC as numerous meltwater injections (up to 30 over 0.015Sv), from remnant glacial lakes

489 on the North American continental margin, into Ungava Bay and other points in the
490 Labrador Sea took place. Six meltwater events (>0.015 Sv, based on 30-day duration)
491 *c.* 7500 to 7000 BP are reported to have occurred. Despite relatively low outflow
492 volumes, the pulsed nature of these freshwater discharges could have led to
493 increased sensitivity of the AMOC, thus altering the degree of NADW production in
494 the Labrador Sea and the degree of heat transport north. Global ocean circulation
495 models suggest that small volumes (<0.06 Sv) of freshwater input are sufficient to
496 cause a shutdown of convection in the Labrador Sea (Rahmstorf, 1995). The
497 existence of substantial meltwater inputs to the Labrador Sea in this period is
498 supported by evidence of abundant *Neogloboquadrin pachyderma* from ocean
499 sediments off Nova Scotia *c.* 7.1 ka BP (Keigwin and Jones, 1995) and a $\delta^{18}O$
500 minimum in the carbonate shells of the foraminifera from these sediments. Both of
501 these features of the ocean record have been interpreted as a consequence of the
502 input of meltwater from either the Great Lakes or Labrador-Ungava region. Evidence
503 of reduced ocean circulation in the North Atlantic Ocean between *c.* 7600-7000 BP
504 can also be inferred from decreasing mean sortable silt sizes from cores in areas of
505 North West Atlantic Bottom Water circulation east of Newfoundland (Hoogakker et
506 al., 2011), in Iceland Scotland Overflow Water (ISOW), in the north eastern Atlantic
507 (Bianchi and McCave, 1999; Figure 7d) and from declining sea surface temperatures

(SSTs) in the Icelandic Sea (Bendle and Rosell Mele, 2007). Sheldon et al. (2015) concluded from dinofagellate records in Eastern Newfoundland that between *c.* 7.2–5.5 ka, SSTs were dominated by cold water sourced from the Arctic via the LC and greater sea ice and iceberg transport resulting from the increased strength and influence of the LC. Dominance of colder waters off the coast must have affected the local climate near the PNDC site, most likely lowering air temperatures and decreasing evapotranspiration, leading to increases in bog water table levels.

The most substantial and abrupt increase in BSW at PNDC occurs *c*. 6600 BP $_{\text{MAR 6472-6759 BP}}$, peaking *c.* 6480 BP $_{\text{MAR 6334-6643 BP}}$ with two further minor increases *c.* 6340 BP $_{\text{MAR 6198-6497 BP}}$ and 6110 BP $_{\text{MAR 6004-6237 BP}}$ (Figure 5). Thereafter, until *c.* 5200 BP the record implies continuity of wet bog surface conditions. There is evidence to suggest that this was also an important period of climate change globally and one of changing AMOC and solar activity (Wanner et al., 2011). Before and during this period further meltwater discharge events from eastern North America (between 7.0 - 6.4 ka) directly into the Labrador Sea and/or Ungava Bay region are reported (Jansson and Kleman 2004). These events may have been large enough to reduce NADW production. Increased advection of cooler surface waters, driven by northerly winds from the Nordic and Labrador Seas, further south into the Atlantic is

527 suggested by a fluctuating but overall increasing level of IRD (Figure 7a) from 7200–
528 5500 BP in the Atlantic Ocean (Bond et al., 2001). In the eastern North Atlantic the
529 importance of this period is clear; from the record of $\delta^{13}C_{Calcite}$ in benthic
530 foraminifera (Oppo et al., 2003) a major reduction in NADW contribution between *c.*
531 6.5 ka and 5.0 ka is inferred and this feature, producing cooler climatic conditions, is
532 considered to be the most pronounced isotopic event in the Holocene section of the
533 record (Figure 7c). SSTs around Iceland are also reported to have reduced
534 substantially at this time (Anderson et al., 2004; Bendle and Rosell Mele, 2007),
535 together with increasing sea ice (Cabedo-Sanz et al., 2016) and strength of nearby
536 ocean currents, such as the ISOW (Bianchi and McCave, 1999) *c.* 6.4 ka (Figure 7d).
537 West of Greenland, periods of cooler sea surface temperatures *c.* 6500 BP have been
538 demonstrated (Hald et al., 2007) and attributed to southward displacement of Arctic
539 waters. The period *c.* 6600-5200 BP was clearly one of abrupt changes in ocean
540 circulation in the N. Atlantic often providing periods of cooler climatic conditions,
541 and these are reflected in the record at PNDC.
542
543 Although evidence of climate change in the neighbouring NDN bog surface wetness
544 record is less clear than that at PNDC, much evidence exists to suggest that this
545 period of changing ocean circulation between *c.* 6700–5200 BP was paralleled by a

546 significant period of change on the Eastern Canadian/American continent. Wetter
547 conditions are evident *c.* 6800 BP to *c.* 6500 BP and *c.* 5800 to 5500 BP in a record
548 derived by Nichols and Huang (2012) of the *Sphagnum*/vascular plant ratio derived
549 from the abundance of biomarker *n* – alkanes from a raised coastal bog to the south
550 of PNDC in Maine, closely reflecting changes seen in the testate amoebae record
551 from PNDC. Sediments of Eastern Lake Ontario in the continental interior also exhibit
552 distinct palaeoenvironmental changes between 6.3 and 6.0 ka ending at 5.0 ka with
553 decreases in % Organic Carbon and % Total Nitrogen and $\delta^{15}N$ (Mc Fadden et al.,
554 2005), reflecting lower lake productivity related to increasing lake levels at this time
555 – an event known as the 'Nipissing rise'. Although often interpreted as a
556 consequence of water moving from the Upper Great Lakes to the Lower Great lakes
557 following isostatic uplift, Booth et al. (2002) noted that a wetter climate prevailed at
558 the time of Nipissing Rise and that increased atmospheric moisture availability was
559 an important factor. Elevated precipitation between *c.* 6600 BP and 5000 BP has also
560 been reconstructed by lake level and pollen records to the east in the St Lawrence
561 lowlands (Muller et al., 2003).
562
563 *Mid - Late Holocene (5000 – 3000 BP)* The PNDC record displays long-term
564 (millennial) lowering of BSW (drier surface conditions) *c.* 5000 – 3000 BP. However,

565 numerous centennial-scale variations occur, some of which can be tied within dating
566 errors to changes in the NDN testate record (e.g. *c.* 5010 $_{\text{MAR 4815-5198 BP}}$, 4500 BP $_{\text{MAR}}$
567 $_{\text{4311 -4669 BP}}$, 4290 BP $_{\text{MAR 4117-4477 BP}}$) and disruption in ocean circulation. Although
568 evident, these changes appear to be of smaller scale compared with those observed
569 earlier in the Holocene *c.* 8000–5200 BP (Figure 5 and 7). Increased NADW
570 production, as interpreted by Oppo et al. (2003) from benthic $\delta^{13}C$, is evident
571 between *c.* 4800–3000 BP, and coincides with the general trend towards lower BSW
572 at the PNDC site (Figure 7c). Decreasing mean sortable silt sizes in sediments,
573 reflecting reduced North West Atlantic Bottom Water circulation east of
574 Newfoundland (Hoogakker et al., 2011), are evident *c.* 4800 BP and *c.* 4500–3900 BP.
575 Less vigorous ocean circulation is also inferred in the eastern North Atlantic since
576 reductions in ISOW (Figure 7d) are recorded *c.* 4800 BP and *c.* 4400 with a low *c.*
577 4200 BP (Bianchi and McCave, 1999) and evidence of increasing IRD *c.* 4800 BP to
578 highs *c.* 4600 BP and *c.* 4200 BP exists (Bond et al., 2001). Increases in IRD,
579 suggesting cooler SSTs are further supported by Andersen et al. (2004) further south
580 in the N. Atlantic and possible slowdowns of NADW. Reports of climate change *c.*
581 4200 BP in the palaeoenvironmental literature are frequent (Mayewski et al., 2004;
582 Booth et al., 2005), with drier conditions evident at mid-lower latitudes and some
583 evidence of increased wetness in more northerly higher latitudes, although the latter

584 appears to be less coherent (Roland et al., 2014). The period around 4200 BP is also
585 often reported as the onset of neoglaciation in the Northern Atlantic region (Larsen
586 et al., 2012; Balascio et al., 2015) as ice caps and glaciers re-advance. A change to
587 cooler conditions (*c.* 4600-4200 BP) has also been recorded in $\delta^{18}O$ from cellulose
588 from *Sphagnum* from Mer Bleu bog in Ontario (Bilali et al., 2013) and $\delta^{18}O$ from lake
589 sediments in Newfoundland (Finkenbinder et al., 2016) point to the onset of wetter
590 conditions *c.* 4300 BP, which is in agreement (Figure 6) with elevated BSW at PNDC
591 and NDN.
592
593 *Late Holocene (3000 BP – present)* Although numerous changes in the PNDC testate
594 amoebae record exist in the Late Holocene, those that can both be replicated by at
595 least one other proxy at PNDC and can be well matched, within dating errors, at
596 NDN, are limited to one event *c.* 2610 $_{\text{MAR 2428-2830 BP}}$ (SI Table 1). The substantial
597 decline in DTWT and the other proxy values *c.* 1480 BP $_{\text{MAR 1219-1755 BP}}$ in PNDC can be
598 replicated within dating errors at NDN but it is at the extreme of the error range,
599 reducing confidence in the coherence of this second event between the two bogs. If
600 changes registered in the testate amoebae record from PNDC are used alone without
601 corroboration with other proxies from PNDC then the reduction in DTWT *c.* 2080 $_{\text{MAR}}$
602 $_{\text{1852-2260 BP}}$ is also evident within dating errors at NDN.

603

604 Substantial evidence of global climate change exists between *c.*2.8–2.6 ka (Wanner
605 et al., 2011) and this has been linked to both ocean circulation and solar activity (van
606 Geel et al., 1999; Chambers et al., 2007). This was a period of reduced NADW
607 production (Oppo, et al., 2003; Bianchi and McCave, 1999), greater IRD (Bond et al.,
608 2001) (Figure 7a) and evidence of migration of arctic waters south (Dourain et al.,
609 2015) and changing atmospheric circulation (O'Brien et al., 1995). Ice caps and
610 glaciers to the north, around Baffin Island (Miller et al., 2005) and Greenland,
611 advanced (Levy et al., 2014; Balasico et al., 2015) and peatland records in
612 Newfoundland (Hughes et al., 2006) and mainland Canada/North America (Nichols
613 and Huang, 2012; Bilali et al., 2013) point towards cooling and/or increased wetness.
614 The PNDC record therefore helps to build the evidence base that suggests there was
615 an increase in atmospheric moisture availability *c.* 2.8 – 2.6 ka on the eastern
616 seaboard of North America at the time of a major global palaeoenvironmental
617 change.

618

619 Conclusions

620 1) Multi-proxy methods have been used to derive a detailed BSW record for the
621 last 8000 years for PNDC in Newfoundland. Comparisons with a neighbouring

622 record at NDN suggests similar timings of water table variability in the period
623 pre-4000 BP, implying a common climate forcing mechanism was a
624 prominent driver of water table level at both sites. However, a common
625 water table response is less clear after 4000 BP, possibly because of
626 insufficient chronological control; however, the possibility that local or
627 autogenic processes (*sensu* Swindles *et al.* 2012) masked low magnitude
628 climate signals in this period cannot be discounted.
629 2) Pronounced evidence of increased BSW in the PNDC record is coherent with
630 meltwater pulses and evidence of reduced NADW activity in the early to mid-
631 Holocene, especially *c.* 7500-6500 BP, suggesting terrestrial responses to
632 substantial ocean circulation changes at this time.
633 3) In the mid-late Holocene the peatland palaeoclimate records appear to be
634 noisier and a distinctive pattern of BSW variability that links to ocean
635 circulation is not clear. There is some apparent coherence between increased
636 BSW *c.* 2610 and 4210 BP in PNDC and evidence of reduced AMOC at these
637 times. These events are two of the high-magnitude palaeoclimate anomalies
638 of the mid to late Holocene. To better recognise the remainder of late
639 Holocene regional peat-based palaeoclimate signal of Eastern Newfoundland
640 improved chronologies pinned with tephras, where possible, and suites of

641 water table constructions from hydrologically-separated sites located within
642 distinct, well-defined spatial climate zones are required.
643
644
645
646
647
648
649
650
651
652
653
654
655
656
657
658
659

660 **Figure Captions**

661 **Figure 1.** Location map of Pound Cove Bog and Nordan's Pond Bog.

662

663 **Figure 2.** Macrofossil diagram for PNDC. Peat Components are derived from
664 averaged quadrat counts (15) under low power magnification (x10). The Leaf Counts
665 are a breakdown of % Identifiable *Sphagnum* and consist of proportions based on a
666 random selection of leaves (>100 per sample interval) identified at high
667 magnification (x400). HCI indices are displayed.

668

669 **Figure 3.** a) Raw and b) detrended humification data for PNDC at 1 cm sampling
670 resolution. Macrofossil zones are superimposed to aid comparison.

671

672 **Figure 4.** Testate amoebae diagram for PNDC. All data are percentages of the total
673 number counted per level. Additional non-testate data such as abundance of *Alona*
674 *rustica* and *Copepod* spermatophores are absolute counts. Transfer function (Booth,
675 2008) depth to water table level reconstructions are displayed.

676

677 **Figure 5.** Comparison of a) macrofossil derived dupont index, b) humification (grey
678 line 1 cm resolution, black line 4cm resolution), c) DTWT from testate data. Grey
679 shading denotes 'wetter periods' based on at least two proxies.
680
681 **Figure 6.** Comparison of PNDC and NDN testate amoebae reconstructed DTWTs.
682 Grey shading represents 95% probability intervals from the age depth model. Black
683 and grey dashed lines between sites records represent events at PNDC that are
684 coherent and well within dating errors at NDN and those that are less robust
685 respectively. SI Table 1 lists details of the dates for each event and associated errors.
686
687 **Figure 7.** Comparison of a) IRD combined record (Bond et al., 2001), b) PNDC DTWT
688 record, c) $\delta^{13}C_{Calcite}$ of benthic foraminifera (Oppo et al., 2003) and d) ISOW record
689 (McCave and Bianchi 1999).
690
691 **Table captions**
692 Table 1. AMS radiocarbon dates from Pound Cove Bog (PNDC) core. Dates were
693 calibrated using IntCal13 (Reimer et al., 2013) within the 'Bacon' computer program
694 (Blaauw and Christen, 2011).
695

References

Aaby B (1976) Cyclic climatic variations in climate over the past 5,500 yrs reflected in raised bogs. *Nature* 263: 281-284.

Aaby B and Tauber H (1974) Rates of peat formation in relation to degree of humification and local environment, as shown by studies of a raised bog in Denmark. *Boreas* 4: 1–17.

Aksenov Y, Bacon S, Coward AC and Penny Holliday N (2010) Polar outflow from the Arctic Ocean: A high resolution model study. *Journal of Marine Systems* 83: 14.

Amesbury MJ, Mallon G, Charman DJ, Hughes PDM, Booth RK, Daley TJ and Garneau M, (2013) Statistical testing of a new testate amoeba-based transfer function for water-table depth reconstruction on ombrotrophic peatlands in north-eastern Canada and Maine, United States. *Journal of Quaternary Science* 28: 27-39.

Amesbury MJ, Swindles GT, Bobrov, A, Charman DJ, Holden J, Lamentowicz M, Mallon G, Mazei Y, Mitchell EAD, Payne RJ, Roland TP, Turner TE and Warner BG

(2016) Development of a new pan-European testate amoeba transfer function for reconstructing peatland palaeohydrology. *Quaternary Science Reviews* 152: 132-151.

Anderson C, Koc N and Moros M (2004) A highly unstable Holocene climate in the subpolar North Atlantic: evidence from diatoms. *Quaternary Science Reviews* 23: 2155-2166.

Balascio NL, D'Andrea WJ and Bradley RS (2015) Glacier response to North Atlantic climate variability during the Holocene. *Climate of the past* 11: 1587-1598.

Banfield CE (1983). Climate. In: South RG (ed) *Biogeography and ecology of the Island of Newfoundland*. The Hague: Dr W. Junk Publishers, pp.37-107.

Barber KE (1981). Peat Stratigraphy and Climate Change: A Palaeoecological Test of the Theory of Cyclic Peat Bog Regeneration. Balkema, Rotterdam, pp. 1–220.

Barber KE (1984). A large capacity Russian-pattern sediment sampler. *Quaternary Newsletter* 44: 28–31.

Barber KE, Chambers FM, Maddy D, Stoneman R and Brew JS (1994) A sensitive high-resolution record of Late Holocene climatic change from a raised bog in northern England. *The Holocene* 4: 198–205.

Barber DC, Dyke A, Hillaire-Marcel C, Jennings AE, Andrews JT, Kerwin MW, Bilodeau G, McNeely R, Southon J, Morehead MD and Gagnon JM (1999) Forcing of the cold event of 8,200 years ago by catastrophic drainage of Laurentide lakes. *Nature* 400: 344–348.

Bastien D-F and Garneau M (1997) Macroscopic identification key of 36 Sphagnum species in eastern Canada. Geological Survey of Canada miscellaneous report 61. *Natural Resources Canada*.

Belyea LR (1996) Separating the effects of litter quality and microenvironment on decomposition rates in a patterned peatland. *Oikos* 77: 529–539.

Bendle JA and Rosell-Melé A (2007) High resolution alkenone sea surface temperature variability on the North Icelandic Shelf: implications for Nordic Seas palaeoclimatic development during the Holocene. *The Holocene* 17: 19-24.

Bianchi GG and McCave IN (1999) Holocene periodicity in North Atlantic climate and deep-ocean flow south of Iceland. *Nature* 397: 515– 517.

Biester H, Knorr KH, Schellekens BA and Hermanns YM (2014) Comparison of different methods to determine the degree of peat decomposition in peat bogs. *Biogeosciences* 11: 2691–2707.

Bilali H, Patterson R and Prokoph A (2013) Holocene Paleoclimate Reconstruction in Eastern Canada: Evidence from delta^{18}O of plant cellulose from the Mer Bleue Bog. *The Holocene* 23: 1260-1271.

Blaauw M and Christen JA (2011) Flexible paleoclimate age-depth models using an autoregressive gamma process. *Bayesian Analysis* 6: 457–474.

Blaauw M and Mauquoy D (2012) Signal and variability within a Holocene peat bog - Chronological uncertainties of pollen, macrofossil and fungal proxies. *Review of Palaeobotony and Palynology* 186: 5-15.

Blackford JJ and Chambers FM (1993) Determining the degree of peat decomposition for peat based palaeoclimatic studies. *International Peat Journal* 5: 7-24.

Blundell A and Barber KE (2005) A 2800-year palaeoclimatic record from Tore Hill Moss, Strathspey, Scotland: the need for a multi-proxy approach to peat-based climate reconstructions. *Quaternary Science Reviews* 24: 1261–1277.

Blundell A, Holden J, and Turner TE (2016) Generating multi-proxy Holocene palaeoenvironmental records from blanket peatlands. *Palaeogeography, Palaeoclimatology, Palaeoecology* 443: 216-229.

Bond G, Kromer B, Beer J, Muscheler R, Evans MN, Showers W, Hoffman S, Lotti-Bond R, Hajdas I and Bonani G (2001) Persistent solar influence on North Atlantic climate during the Holocene. *Science* 294: 2130–2136.

Booth RK (2008) Testate amoebae as proxies of mean annual water-table depth in Sphagnum-dominated peatlands of North America. *Journal of Quaternary Science* 23: 43–57.

Booth RK and Jackson ST (2002) Paleoecology of a Northern Michigan Lake and the Relationship among Climate, Vegetation, and Great Lakes Water Levels. *Quaternary Research* 57: 120–130.

Booth RK, Jackson ST, Forman SL, Kutzbach JE, Bettis III EA, Kreig J and Wright DK (2005) A severe centennial-scale drought in mid-continental North America 4200 years ago and apparent global linkages. *The Holocene* 15: 321-328.

Cabedo-Sanz P, Belt ST, Jennings A., Andrews JT and Geirsdóttir, Á. (2016) Variability in drift ice export from the Arctic Ocean to the North Icelandic Shelf over the last 8,000 years: a multi-proxy evaluation. *Quaternary Science Reviews* 146: 99-115.

Carlson AE, LeGrande AN, Oppo DW, Came RE, Schmidt GA, Anslow FS, Licciardi JM and Obbink EA (2008) Rapid early Holocene deglaciation of the Laurentide Ice Sheet, *Nature Geoscience* 1: 620-624.

Caseldine C, Baker A, Charman DJ and Hendon D (2000). A comparative study of optical properties of NaOH peat extracts: implications for humification studies. *The Holocene* 10: 649-658.

Chambers FM, Mauquoy D, Brain SA, Blaauw M and Daniell JRG (2007) Globally synchronous climate change 2800 years ago: proxy data from peat in South America. *Earth and Planetary Science Letters* 253: 439–444.

Chambers FM, Booth RK, De Vleeschouwer F, Lamentowicz M, Le Roux G, Mauquoy D, Nichols JE and van Geel B (2012) Development and refinement of proxy-climate indicators from peats. *Quaternary International* 268: 21–33.

Charman DJ, Blundell A and ACCROTELM members (2006) A new European testate amoebae transfer function for palaeohydrological reconstruction on ombrotrophic peatlands. *Journal of Quaternary Science* 22: 209-221.

Charman DJ, Hendon D and Woodland WA (2000) *The Identification of Testate Amoebae (Protozoa: Rhizopoda) in Peats*. London: Quaternary Research Association.

Charman DJ and Warner BG (1997) The ecology of testate amoebae (Protozoa : Rhizopoda) in oceanic peatlands in Newfoundland, Canada: modelling hydrological relationships for palaeoenvironmental reconstruction. *Ecoscience* 4: 555–562.

Coulson JC and Butterfield J (1978) An investigation of the biotic factors determining the rates of plant decomposition on blanket bog. *Journal of Ecology* 66: 631-650.

Daley TJ and Barber KE (2012) Multi-proxy Holocene palaeoclimate records from Walton Moss, northern England and Dosenmoor, northern Germany, assessed using three statistical approaches. *Quaternary International* 268: 111–127.

Daley TJ, Barber KE, Hughes PDM, Loader NJ, Leuenberger MC, Street-Perrott FA (2016) The 8.2 ka BP event in north eastern North America - first combined oxygen- and hydrogen- isotopic data in peat from Newfoundland, *Journal of Quaternary Science* 31 (4): 416-425.

Daley TJ**,** Street-Perrott FA, Loader NJ, Barber KE, Hughes PDM, Fisher EH and Marshall JD (2009) Terrestrial climate signal of the "8200-yr cold event" in the Labrador Sea region. *Geology* 37: 831-834.

Daley TJ, Thomas ER, Holmes JA, Street-Perrott FA, Chapman MR, Tindall JC, Valdes PJ, Loader NJ, Marshall JD, Wolff EW, Hopley PJ, Atkinson T, Barber KE, Fisher EH,

Robertson I, Hughes PDM and Roberts CN (2011) The 8200yr BP cold event in stable isotope records from the North Atlantic region. *Global and Planetary Change* 79: 288–302.

Damman AWH (1980) Ecological and floristic trends in the ombrotrophic bogs of eastern North America. In Gehu JM (ed) *La végétation dessols tourbeux*. Colloq. Phytosoc. (Lille 1978) 7. J. Cramer, Vaduz, pp. 61-79.

Daniels RE and Eddy A (1990) *A Handbook of European Sphagna*. Natural Environment Research Council: Swindon.

Dourain M, Elliot M, Noble SR, Moreton SG, Long D, Sinclair D, Henry L-A and Roberts JM (2015) North Atlantic ecosystem sensitivity to Holocene shifts in Meridional Overturning Circulation. *Geophysical Research Letters* 10.1002/2015GL065999.

Drinkwater KF (1996) Atmospheric and Oceanic Variability in the Northwest Atlantic during the 1980s and Early 1990s. *Journal of Northwestern Atlantic Fisheries Science* 18: 77–97.

Dupont LM (1986) Temperature and rainfall variation in the Holocene based on comparative palaeoecology and isotope geology of a hummock and a hollow. *Review of Palaeobotany and Palynology* 48: 71–159.

Dyke AS and Prest VK (1987) Late Wisconsinan and Holocene history of the Laurentide Ice Sheet. *Geographie Physique et Quaternaire* 41 : 237-263.

Elmore A, Wright JD and Southon J (2015) Continued meltwater influence on North Atlantic Deep Water instabilities during the early Holocene. *Marine Geology* 360: 17-24.

Finkenbinder MS, Abbott MB, Steinman B (2016) Holocene climate change in Newfoundland reconstructed using oxygen isotope analysis of lake sediment cores. Global and Planetary Change 143:251-261.

Frantantoni PS and McCartney MS (2010) Freshwater export from the Labrador Current to the North Atlantic Current at the Tail of the Grand Banks of Newfoundland. *Deep-Sea Research* 57: 258-283.

Gałka M, Miotk-Szpiganowicz G, Marczewska M, Barabach J, van der Knaap W, Lamentowicz M (2015) Palaeoenvironmental changes in Central Europe (NE Poland) during the last 6200 years reconstructed from a high-resolution multi-proxy peat archive. The *Holocene* 25: 421–434.

Hald M, Andersson C, Ebbesen H, Jansen E, Klitgaard-Kristensen D, Risebrobakken B, Salomonsen GR, Sarnthein M, Sejrup HP and Telford RJ (2007) Variations in temperature and extent of Atlantic water in the northern North Atlantic during the Holocene. *Quaternary Science Reviews* 26: 3423-3440.

Hoogakker BAA, Chapman MR, McCave IN, Hillaire-Marcel C, Ellison CRW, Hall IR and Telford RJ (2011) Dynamics of North Atlantic Deep Water masses during the Holocene. *Paleoceanography* 26: PA4214.

Hughes PDM, Blundell A, Charman DJ, Bartlett S, Daniell JRG, Wojatschke A and Chambers FM (2006) A 8500 cal. year multiproxy climate record from a bog in eastern Newfoundland: contributions of meltwater discharge and solar forcing. *Quaternary Science Reviews* 25: 1208–1227.

Hughes PDM, Mallon G, Essex H, Amesbury MJ, Charman DJ, Blundell A, Chambers FM, Daley TJ and Mauquoy D (2012) The use of k-values to examine plant pigmentation 'species signals' in a peat humification record from Newfoundland. *Quaternary International* 268: 156–165.

Jansson KN and Kleman J (2004) Early Holocene glacial lake meltwater injections into the Labrador Sea and Ungava Bay. *Palaeoceanography* 19: PA1001.

Johnson LC and Damman AWH (1991) Species-controlled Sphagnum decay on a South Swedish raised bog. *Oikos* 61: 234-242.

Jones EP and Anderson LG (2008) Is the global conveyor belt threatened by Arctic Ocean fresh water outflow? In: Dickson RR, Meincke J and Rhines P (eds) *Arctic-Subarctic Ocean Fluxes*. Springer, pp.385–404.

Keigwin LD and Jones GA (1995) The marine record of deglaciation from the continental margin off Nova Scotia, *Paleoceanography* 10: 973-985.

Kilian MR, Van der Plicht J and Van Geel B (1995) Dating raised bogs: new aspects of AMS ^{14}C Wiggle matching, a reservoir effect and climatic change. *Quaternary Science Reviews* 14: 959–966.

Kuhlbrodt T, Rahmstorf S, Zickfeld K, Vikebø FB, Sundby S, Hofmann M, Link PM, Bondeau A, Cramer W and Jaeger C (2009) An Integrated Assessment of changes in the thermohaline circulation. *Climatic Change* 96: 489-537.

Lacourse T and Davies MA (2015) A multi-proxy peat study of Holocene vegetation history, bog development, and carbon accumulation on northern Vancouver Island, Pacific coast of Canada. *The Holocene* 25: 1165-1178.

Larsen D, Miller GH, Geirsdóttir Á and Ólafsdóttir S (2012) Non-linear Holocene climate evolution in the North Atlantic: a high-resolution, multi-proxy record of glacier activity and environmental change from Hvítárvatn, central Iceland. *Quaternary Science Reviews* 39: 14-25.

Levy LB, Kelly MA, Lowell TV, Hall BL, Hempel LA, Honsaker WM, Lusas AR, Howley JA and Axford YL (2014) Holocene fluctuations of Bregne ice cap, Scoresby Sund, east

Greenland: a proxy for climate along the Greenland Ice Sheet margin. *Quaternary Science Reviews* 92: 357–368.

Limpens J and Berendse F (2003) How litter quality affects mass Loss and N loss from decomposing *Sphagnum*. *Oikos* 103: 537–547.

Mackay H, Hughes PDM, Jensen BJL, Langdon PG, Pyne-O'Donnell SDF, Plunkett G, Froese DG, Coulter S, Gardner JE (2016). A mid to late Holocene cryptotephra framework from eastern North America. *Quaternary Science Reviews* 132: 101-113.

Marshall J, Kushnir Y, Battisti D, Chang P, Czaja A, Dickson R, Hurrell J, McCartney M, Saravanan R and Visbeck M (2001) North Atlantic climate variability: Phenomena, impacts and mechanisms. *International Journal of Climatology* 21: 1863–1898.

Marshall J and Schott F (1999) Open-ocean convection: observations, theory, and models. *Reviews of Geophysics* 37: 1-64.

Mathijssen PJH, Valiranta M, Korrensalo A, Alekseychik P, Vesala T, Rinne J, Tuittila E-S (2016) Reconstruction of Holocene carbon dynamics in a large boreal peatland complex, southern Finland. *Quaternary Science Reviews* 142: 1-15.

Mayewski PA, Rohling EE, Stager JC, Karlen W, Maasch KA, Meeker LD, Meyerson EA, Gasse F, van Kreveld S, Holmgren K, Lee-Thorp J, Rosqvist G. Rack F, Staubwasser M, Schneider RR and Steig EJ (2004) Holocene climate variability. *Quaternary Research* 62: 243-255.

Mc Fadden MA, Patterson WP, Mullins HT and Anderson WT (2005) Multi-proxy approach to long- and short-term Holocene climate-change: evidence from eastern Lake Ontario. *Journal of Paleoecology* 33: 371-391.

Miller GH, Wolfe AP, Briner JP, Sauer PE and Nesje A (2005) Holocene glaciation and climate evolution of Baffin Island, Arctic Canada. *Quaternary Science Reviews* 24: 1703–1721.

Mitchell EAD, Payne RJ, Lamentowicz M. (2008) Potential implications of different preservation of testate amoebae shells for paleoenvironmental reconstruction in peatlands. *Journal of Paleolimnology* 40: 603-618. Doi:10.1007/s10933-007-9185-z

Morris PJ, Baird AJ, Young DM and Swindles GT (2015) Untangling climate signals from autogenic changes in long-term peatland development. *Geophysical Research Letters* 42: 10,788–10,797.

Muller SD, Richard PJH, Guiot J, de Beaulieu JL and Forti D (2003) Postglacial climate in the St. Lawrence lowlands, southern Quebec: pollen and lake-level evidence. *Palaeogeography, Palaeoclimatology, Palaeoecology* 193: 51-72.

Nichols JE and Huang Y (2012) Hydroclimate of the northeastern United States is highly sensitive to solar forcing. *Geophysical Research Letters* 39: L04707.

Novenko EY, Tsyganov AN, Volkova EM, Babeshko KV, Lavrentiev NV, Payne RJ and Mazei YA (2015) The Holocene paleoenvironmental history of central European Russia reconstructed from pollen, plant macrofossil, and testate amoeba analyses of the Klukva peatland, Tula region. *Quaternary Research* 83: 459-468.

O'Brien SR, Mayewski PA, Meeker DL, Meese DA, Twickler MS. and Whitlow SI (1995) Complexity of Holocene Climate as reconstructed from a Greenland Ice Core. *Science* 270: 1962-1964.

Oppo DW, McManus JF and Cullen JL (2003) Deepwater variability in the Holocene epoch. *Nature* 422: 277-278.

Payne RJ and Mitchell EAD (2009) How many is enough? Determining optimal count totals for ecological and palaeoecological studies of testate amoebae. *Journal of Paleolimnology* 42: 483–495.

Payne RJ, Lamentowicz M and Mitchell EAD (2010) The perils of taxonomic inconsistency in quantitative palaeoecology: experiments with testate amoeba data. *Boreas* 40: 15-27.

Payne RJ, Telford RJ, Blackford JJ, Blundell A, Booth RK, Charman DJ, Lamentowicz L, Lamentowicz M, Mitchell EAD, Potts G, Swindles GT, Warner BG and Woodland W

(2012) Testing peatland testate amoeba transfer functions: Appropriate methods for clustered training-sets. *The Holocene* 22: 819-825.

Peros MC, Chan K, Magnan G, Ponsford L, Carroll J, McCloskey T (2016). A 9600-year History of Water Table Depth, Vegetation, and Fire Inferred from a Raised Peat Bog, Prince Edward Island, Canadian Maritimes. *Journal of Quaternary Science* 31: 512-525.

Pyne-O'Donnel S, Hughes PDM, Froese DG, Jensen BJL, Kuehn SC, Mallon G, Amesbury MJ, Charman DJ, Daley TJ, Loader NJ, Mauquoy D, Street-Perrott FA and Woodman-Ralph J (2012) High-precision ultra-distal Holocene tephrochronology in North America. *Quaternary Science Reviews* 52: 6-11.

R Core Team (2012) R: A Language and Environment for Statistical Computing. R Foundation for Statistical Computing, Vienna, Austria.

Rahmstorf S (1995) Bifurcations of the Atlantic thermohaline circulation in response to changes in the hydrological cycle. *Nature* 378: 145–149.

Rahmstorf S, Box JE, Feulner G, Mann ME, Robinson A, Rutherford S and Schaffernicht EJ (2015) Exceptional twentieth-century slowdown in Atlantic Ocean overturning circulation. *Nature Climate Change* 5: 475-480.

Reimer PJ, Bard E, Bayliss A, Beck JW, Blackwell PG, Bronk Ramsey C, Buck CE, Edwards RL, Friedrich M, Grootes PM, Guilderson TP, Haflidason H, Hajdas I, Hatté C, Heaton TJ, Hoffmann DL, Hogg AG, Hughen KA, Kaiser KF, Kromer B, Manning SW, Niu M, Reimer RW, Richards DA, Scott ME, Southon JR, Turney CSM, van der Plicht, J (2013) IntCal13 and Marine13 radiocarbon age calibration curves 0-50,000 yr cal BP. *Radiocarbon* 55: 1869-1887

Robertson A (2000) Flora of Peatland Ecosystems in Newfoundland and Labrador and the French Islands of St. Pierre and Miquelon. St. John's Newfoundland.

Rogerson RJ (1983) Geological evolution. In: South RG (ed.) *Biogeography and ecology of the island of Newfoundland*. The Hague: Dr W. Junk Publishers, pp.5-37.

Roland TP, Caseldine CJ, Charman DJ, Turney CSM and Amesbury MJ (2014) Was there a '4.2ka event' in Great Britain and Ireland? Evidence from the peatland record. *Quaternary Science Reviews* 83: 11-27.

Rossby T (1999) On gyre interactions. *Deep-Sea Research* 46: 139-164.

Sheldon CM, Seidenkrantz MS, Frandsen P, Jacobsen HV, Van Nieuwenhove N, Solignac S, Pearce C, Palitzsch MG and Kuijpers A (2015) Variable influx of West Greenland Current water into the Labrador Current through the last 7200 years - a multiproxy record from Trinity Bay (NE Newfoundland). *Arktos – Arctic Geoscience.* doi: 10.1007/s41063-015-0010-z.

Sicre M-A, Weckström K, Seidenkrantz M-S, Kuijpers A, Benetti M, Masse G, Ezat U, Schmidt S, Bouloubassi I, Olsen J and Khodri M (2014) Labrador Current variability over the last 2000 years. *Earth and Planetary Science Letters* 400: 26-32.

Smith AJE (2004) *The Moss Flora of Britain and Ireland*. Second Edition, Cambridge: Cambridge University Press.

Stouffer RJ, Yin J, Gregory JM, Dixon KW, Spelman MJ, Hurlin W, Weaver AJ, Eby M, Flato G M, Hasumi H, Hu A, Jungclaus JH, Kamenkovich IV, Levermann A, Montoya M, Murakami S, Nawrath, S, Oka A, Peltier WR, Robitaille DY, Sokolov A, Vettoretti G, and Weber SL (2006) Investigating the causes of the response of the thermohaline circulation to past and future climate changes. *Journal of Climate* 19: 1365–1387.

Swindles GT and Roe HM (2007) Examining the dissolution characteristics of testate amoebae (Protozoa: Rhizopoda) in low pH conditions: implications for peatland palaeoclimate studies. *Palaeogeography, Palaeoecology, Palaeoclimatology* 252: 486–496.

Swindles GT, Morris PJ, Baird AJ, Blaauw M and Plunkett G (2012) Ecohydrological feedbacks confound peat-based climate reconstructions. *Geophysical Research Letters* 39: L11401.

Swindles GT, Holden J, Raby C, Turner TE, Blundell A, Charman DJ, Menberu MW and Kløve B (2015) Testing peatland water-table depth transfer functions using high resolution hydrological monitoring data. *Quaternary Science Reviews* 120: 107–117.

Swingedouw D (2015) Oceanography: Fresh news from the Atlantic. *Nature* doi:10.1038/nclimate2626.

Telford RJ and Birks HJB (2009) Evaluation of transfer functions in spatially structured environments. *Quaternary Science Reviews* 28: 1309-1316.

Telford RJ and Birks HJB (2011) A novel method for assessing the statistical significance of quantitative reconstructions inferred from biotic assemblages. *Quaternary Science Reviews* 30: 1272–1278.

Turner TE, Swindles GT and Roucoux KH (2014) Late Holocene ecohydrological and carbon dynamics of a UK raised bog: impact of human activity and climate change. *Quaternary Science Reviews* 84: 65–85.

van Geel B, Raspopov OM, Renssen H, van der Plicht J, Dergachev VA and Meijer HAJ (1999) The role of solar forcing upon climate change. *Quaternary Science Reviews* 18: 331-338.

Väliranta M, Blundell A, Charman DJ, Karofeld E, Korhola A, Sillasoo U, Tuittila E-S (2012) Reconstructing peatland water tables using transfer functions for plant macrofossils and testate amoebae: A methodological comparison. *Quaternary International* 268: 34-43.

Waddington JM, Morris PJ, Kettridge N, Granath G, Thompson DK and Moore PA (2015) Hydrological feedbacks in northern peatlands. *Ecohydrology* 8: 113–127.

Wagner AJ, Morrill C, Otto-Bliesner BL, Rosenbloom N and Watkins KR (2013) Model support for forcing of the 8.2 ka event by meltwater from the Hudson Bay ice dome. *Climate Dynamics* 41: 2855. doi:10.1007/s00382-013-1706-z

Wanner H, Solomina O, Grosjean M, Ritz SP and Jetel M (2011) Structure and origin of Holocene cold events. *Quaternary Science Reviews* 30: 3109-3123.

Weaver AJ, Sedláček J, Eby M, Alexander K, Crespin E, Fichefet T, Philippon-Berthier G, Joos F, Kawamiya M, Matsumoto K, Steinacher M, Tachiiri K, Tokos K, Yoshimori M and Zickfeld K (2012) Stability of the Atlantic meridional overturning circulation: A

model intercomparison. *Geophysical Research Letters* 39, L20709, doi:10.1029/2012GL053763.

Wells ED (1981) Peatlands of eastern Newfoundland: distribution, morphology, vegetation, and nutrient status. Canadian Journal of Botany 59, 1978-1997.

Wells ED and Pollett FC (1983) "Peatlands". ln: South GR (ed.) *Biogeography and Ecology of the island of Newfoundland*. The W. Junk Publisher, Hague, The Netherlands, pp. 207-267.

Wilmshurst JM, Wiser SK and Charman DJ (2003) Reconstructing Holocene water tables in New Zealand using testate amoebae: differential preservation of tests and implications for the use of transfer functions. *The Holocene* 13: 61–72.

Woodland WA, Charman DJ and Sims PC (1998) Quantitative estimates of water tables and soil moisture in Holocene peatlands from testate amoebae. *The Holocene* 8: 261–273.

Yeloff D and Mauquoy D (2006) The influence of vegetation composition on peat humification: implications for palaeoclimatic studies. *Boreas* 35: 622–673.

Figure 1.

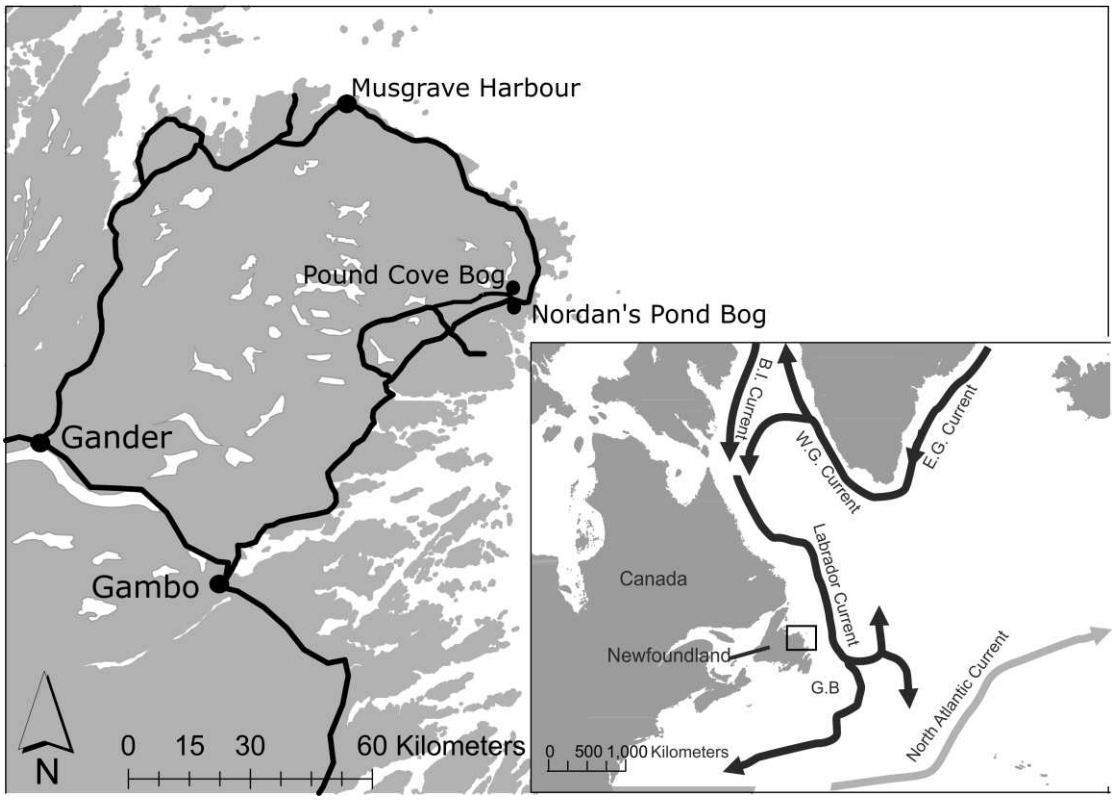
Musgrave Harbour
Pound Cove Bog
Nordan's Pond Bog
Gander
Gambo
N
0 15 30
60 Kilometers
B.I. Current
W.G. Current
E.G. Current
Labrador Current
Canada
Newfoundland
G.B
North Atlantic Current
0 500 1,000 Kilometers

Figure 2

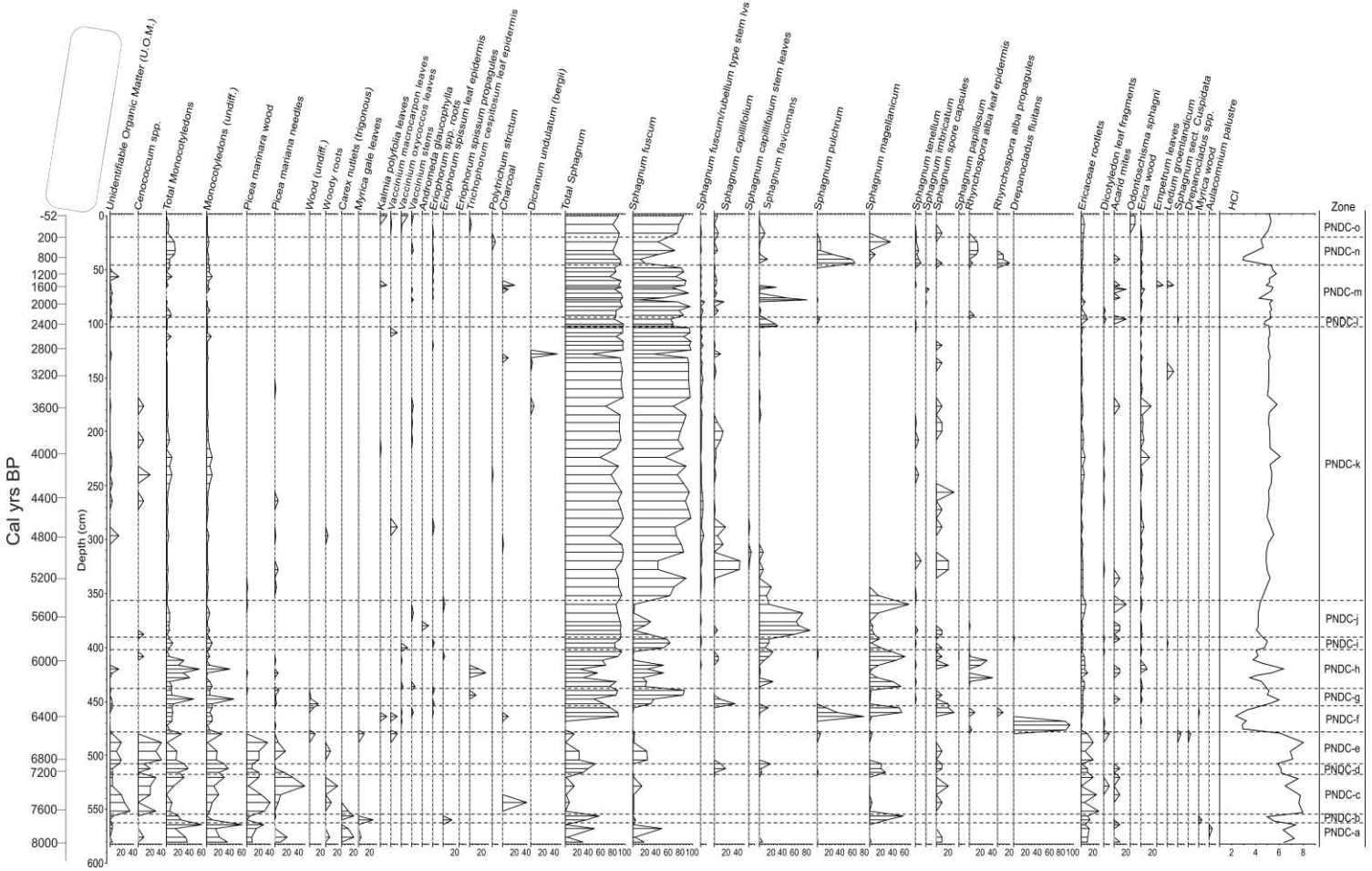
Cal yrs BP
Depth (cm)
Unidentifiable Organic Matter (U.O.M.)
Cenococcum spp.
Total Monocotyledons
Monocotyledons (undiff.)
Picea marinara wood
Picea mariana needles
Wood (undiff.)
Woody roots
Carex nutlets (trigonous)
Myrica gale leaves
Kalmia polyfolia leaves
Vaccinium macrocarpon leaves
Vaccinium stamens
Andromeda glaucophylla leaves
Eriophorum spp. roots
Eriophorum spissum leaf epidermis
Trichophorum cespitosum leaf epidermis
Polytrichum strictum
Charcoal
Dicranum undulatum (bergii)
Total Sphagnum
Sphagnum fuscum
Sphagnum fuscum/rubellum type stem lvs
Sphagnum capillifolium
Sphagnum capillifolium stem leaves
Sphagnum flavicomans
Sphagnum pulchrum
Sphagnum magellanicum
Sphagnum tenellum
Sphagnum imbricatum
Sphagnum spore capsules
Sphagnum papillosum
Rhynchospora alba leaf epidermis
Rhynchospora alba propagules
Drepanocladus fluitans
Ericaceae rootlets
Dicotyledon leaf fragments
Acarid mites
Odontoschisma sphagni
Erica wood
Empetrum leaves
Ledum groenlandicum
Sphagnum leaves Cuspidata
Drepanocladus spp.
Myrica wood
Aulacommium palustre
HCl
Zone
PNDC-o
PNDC-n
PNDC-m
PNDC-l
PNDC-k
PNDC-j
PNDC-i
PNDC-h
PNDC-g
PNDC-f
PNDC-e
PNDC-d
PNDC-c
PNDC-b
PNDC-a

Figure 3

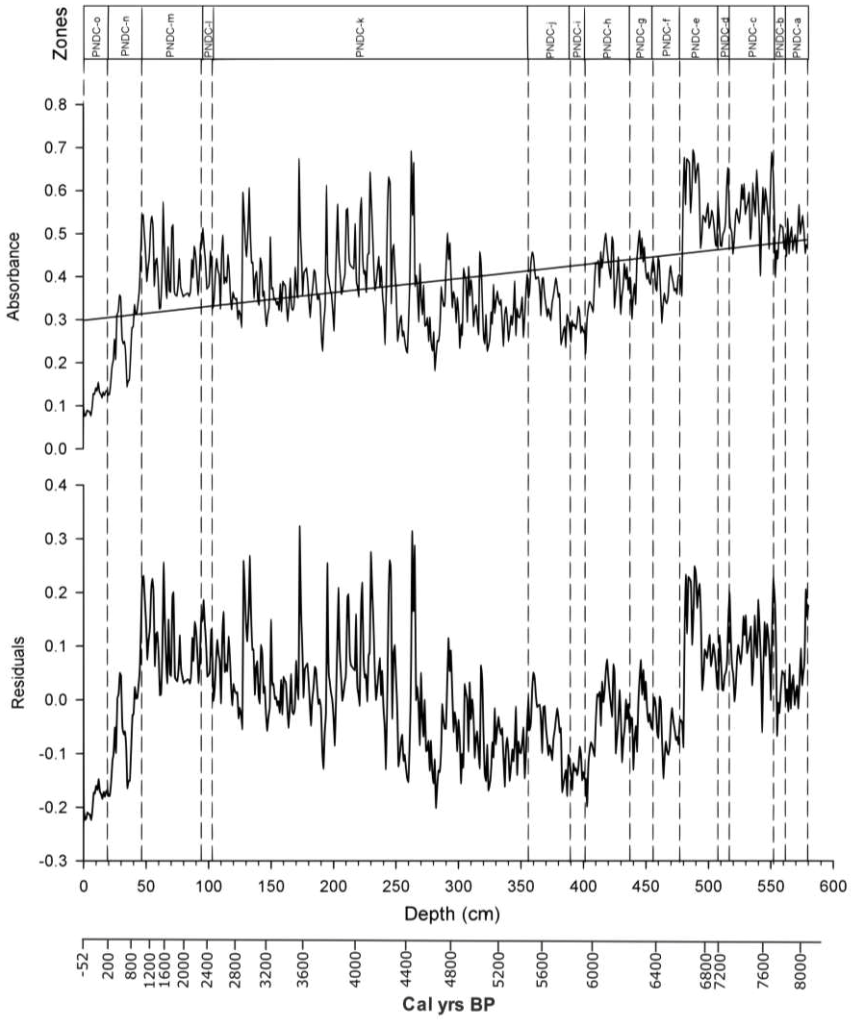
Zones
PNDC-o
PNDC-n
PNDC-m
PNDC-l
PNDC-k
PNDC-j
PNDC-i
PNDC-h
PNDC-g
PNDC-f
PNDC-e
PNDC-d
PNDC-c
PNDC-b
PNDC-a
Absorbance
Residuals
Depth (cm)
Cal yrs BP

Figure 4

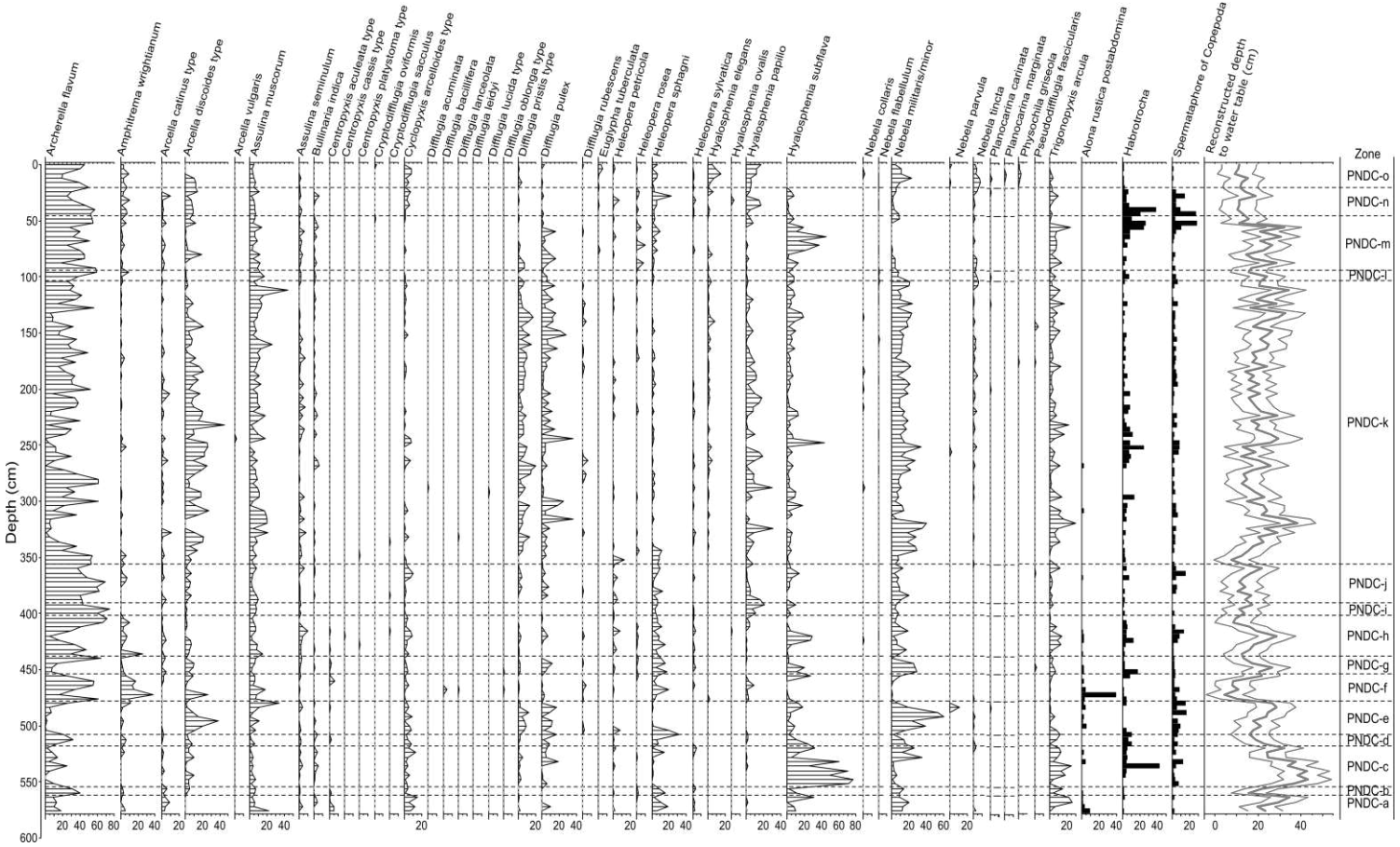
Archerella flavum
Amphitrema wrightianum
Arcella catinus type
Arcella discoides type
Arcella vulgaris
Assulina muscorum
Assulina seminulum
Bullinaria indica
Centropyxis aculeata type
Centropyxis cassis type
Centropyxis platystoma type
Cryptodifflugia oviformis
Cryptodifflugia sacculus
Cyclopyxis arcelloides type
Difflugia acuminata
Difflugia bacillifera
Difflugia lanceolata
Difflugia leidyi
Difflugia lucida type
Difflugia oblonga type
Difflugia pristis type
Difflugia pulex
Difflugia rubescens
Euglypha tuberculata
Heleopera petricola
Heleopera rosea
Heleopera sphagni
Heleopera sylvatica
Hyalosphenia elegans
Hyalosphenia ovalis
Hyalosphenia papilio
Hyalosphenia subflava
Nebela collaris
Nebela flabellulum
Nebela militaris/minor
Nebela parvula
Nebela tincta
Planocarina carinata
Planocarina marginata
Physochila griseola
Pseudodifflugia fascicularis
Trigonopyxis arcula
Alona rustica postabdomina
Habrotrocha
Spermataphore of Copepoda
Reconstructed depth to water table (cm)
Depth (cm)
Zone
PNDC-o
PNDC-n
PNDC-m
PNDC-l
PNDC-k
PNDC-j
PNDC-i
PNDC-h
PNDC-g
PNDC-f
PNDC-e
PNDC-d
PNDC-c
PNDC-b
PNDC-a

Figure 5

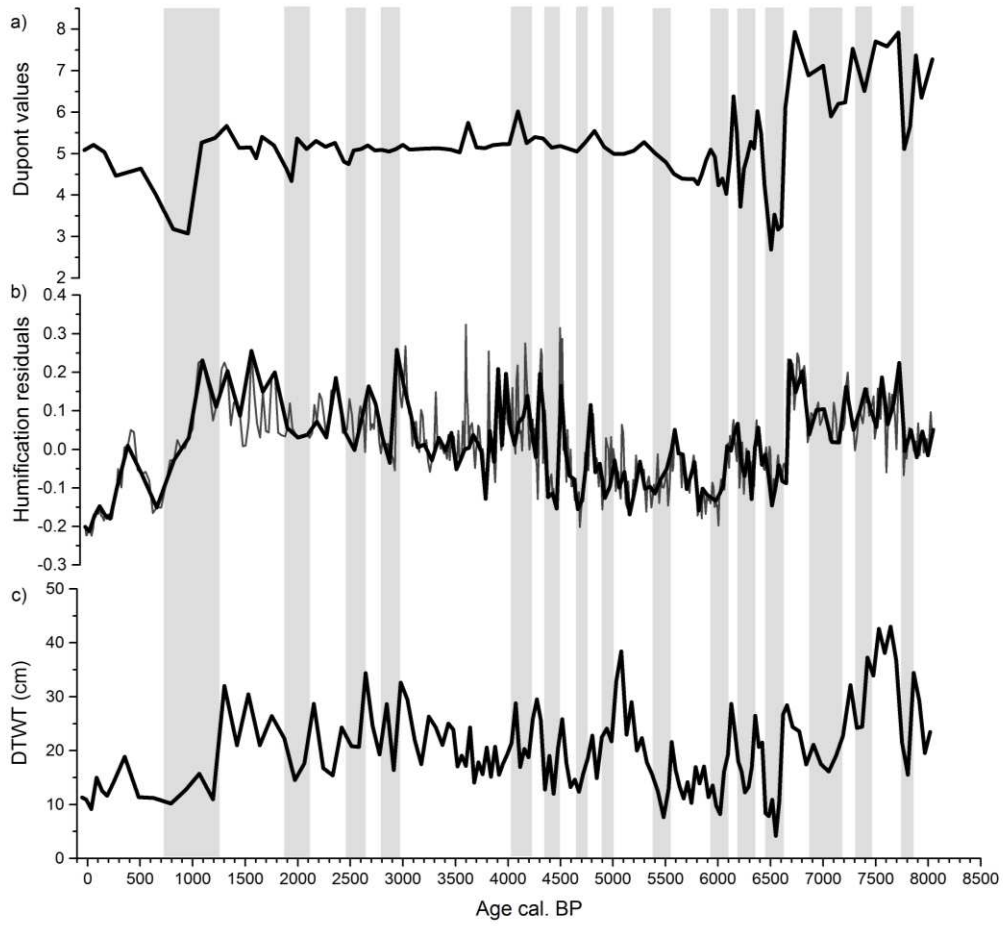
a)
Dupont values
b)
Humification residuals
c)
DTWT (cm)
Age cal. BP

Figure 6

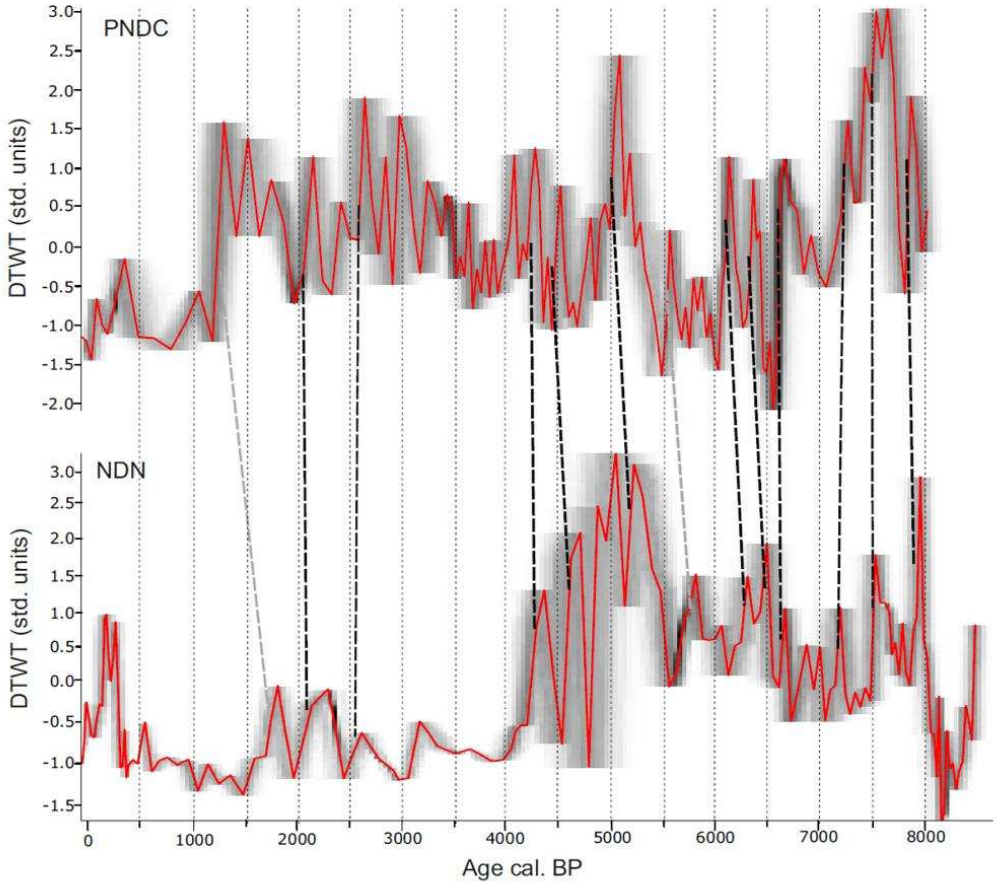
PNDC
NDN
DTWT (std. units)
DTWT (std. units)
3.0
2.5
2.0
1.5
1.0
0.5
0.0
-0.5
-1.0
-1.5
-2.0
0
1000
2000
3000
4000
5000
6000
7000
8000
Age cal. BP

Figure 7

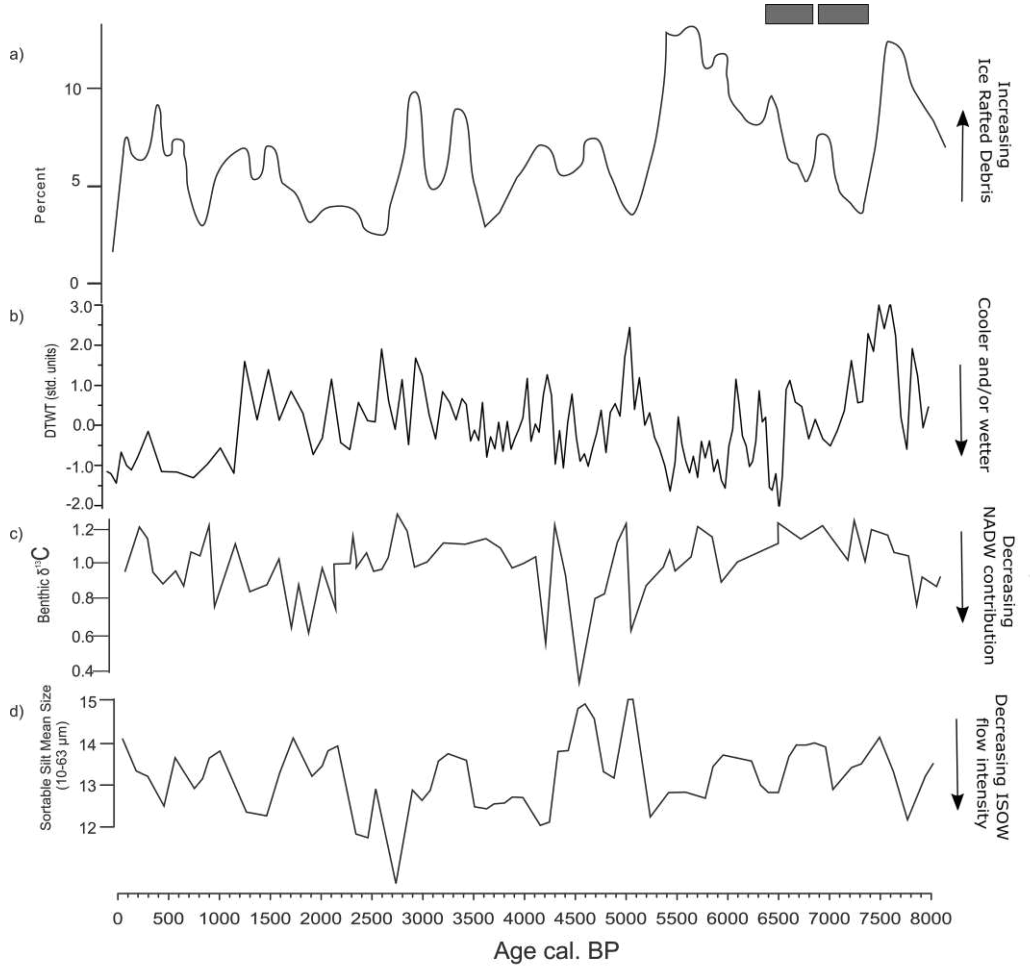
a)
Percent
10
5
0
Increasing
Ice Rafted Debris
b)
DTWT (std. units)
3.0
2.0
1.0
0.0
-1.0
-2.0
Cooler and/or wetter
c)
Benthic δ13C
1.2
1.0
0.8
0.6
0.4
Decreasing
NADW contribution
d)
Sortable Silt Mean Size
(10-63 µm)
15
14
13
12
Decreasing ISOW
flow intensity
0 500 1000 1500 2000 2500 3000 3500 4000 4500 5000 5500 6000 6500 7000 7500 8000
Age cal. BP

Table 1

Lab no.	Depth (cm)	Material	AMS RC date BP (uncal.)	1 δ error	Cal. range (2δ) BP
SUERC-11763	24	*Sphagnum*	144	35	2 - 282
SUERC-11764	48	*Sphagnum*	1157	35	979 - 1172
SUERC-542	80	*Sphagnum*	2027	26	1899 - 2056
SUERC-11765	104	*Sphagnum*	2479	35	2366 - 2717
SUERC-11767	160	*Sphagnum*	3235	35	3383 - 3556
SUERC-543	216	*Sphagnum*	3660	41	3874 - 4139
BETA-195385	291	*Sphagnum*	4140	40	4535 - 4824
SUERC-11768	352	*Sphagnum*	4753	35	5330 - 5587
SUERC-11769	392	*Sphagnum*	5113	35	5749 - 5926
BETA-195386	412	*Sphagnum*	5320	40	5991 - 6263
SUERC-544	480	*Sphagnum*	5727	32	6442 - 6633
SUERC-11770	520	*Sphagnum*	6345	36	7172 - 7413
SUERC-545	576	*Sphagnum*	7222	39	7964 - 8159

Supplementary Figure and Table captions

Supplementary Figure 1. 'Bacon' based Bayesian age-depth model (Blaauw and Christen, 2011) for the core from PNDC. The three upper charts from left to right denote the stability of the Markov Chain Monte Carlo iterations (>1000 iterations), and the prior (green line) and posterior (grey shading) for accumulation rate and memory employed. For the lower chart: blue shading shows age distributions of calibrated AMS ^{14}C dates and grey shading denotes the posterior age-depth model bounded by grey dots showing the 95% probability intervals of the model.

Supplementary Figure 2. Scatterplots showing comparisons between standardised proxy values from PNDC.

Supplementary Figure 3. 'Bacon' based Bayesian age-depth model (Blaauw and Christen, 2011) for the core from NDN. The three upper charts from left to right denote the stability of the Markov Chain Monte Carlo iterations (>1000 iterations), and the prior (green line) and posterior (grey shading) for accumulation rate and memory employed. For the lower chart: blue shading shows age distributions of calibrated AMS ^{14}C dates and grey shading denotes the posterior age-depth model bounded by grey dots showing the 95% probability intervals of the model.

Supplementary Table 1. Dates and error ranges of prominent changes to reduced HCI, reconstructed DTWTs and levels of humification implying elevated water tables at PNDC. Grey shading denotes replication of changes by at least two proxies at PNDC. Changes to elevated water tables at NDN as derived from testate amoebae are listed and are in bold when they are well within the radiocarbon errors of those from the PNDC testate amoebae data.

Supplementary Table 2. Coefficient of determination and associated *p* values in parentheses for each standardised proxy and testate transfer function.

Supplementary Figure 1

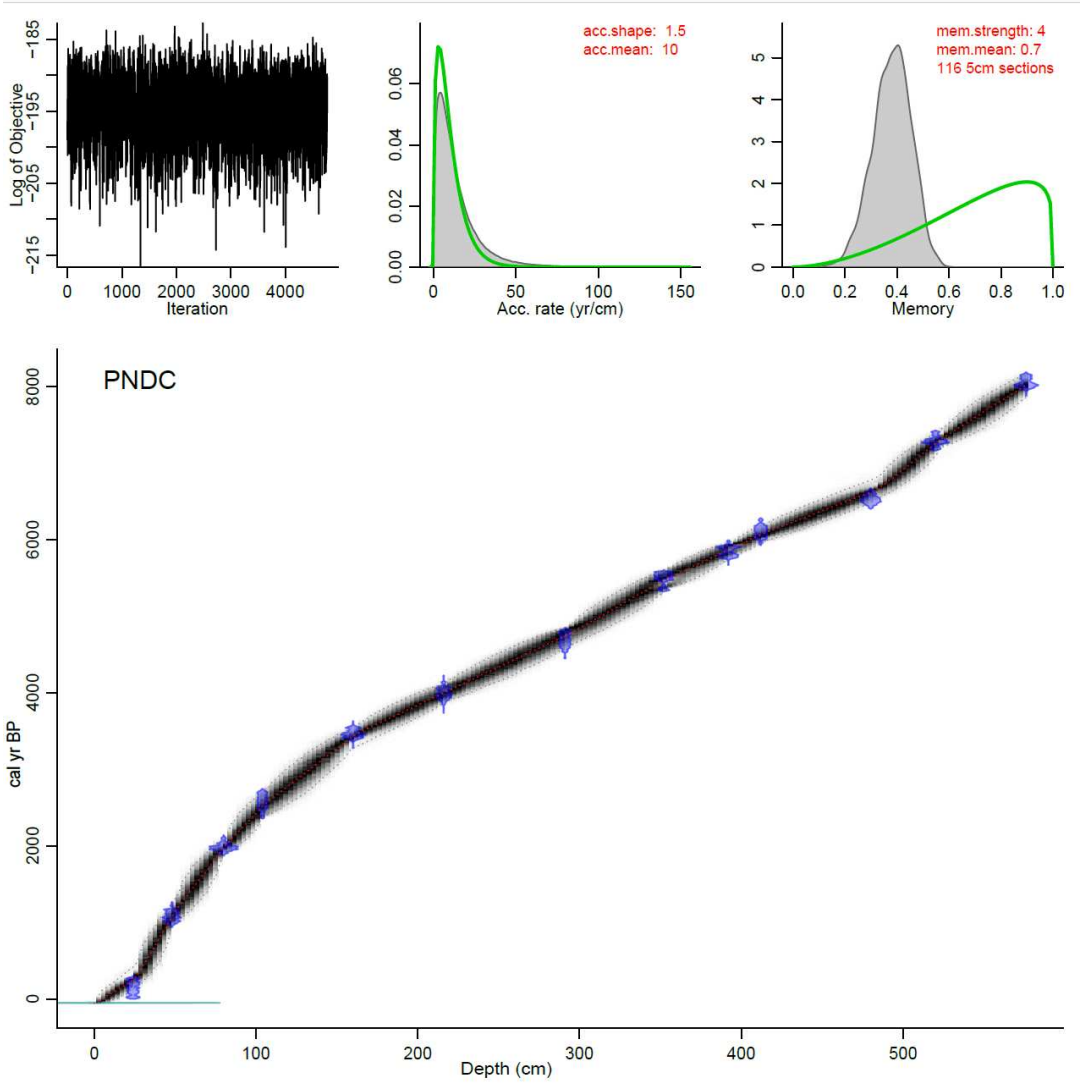

Supplementary Figure 2

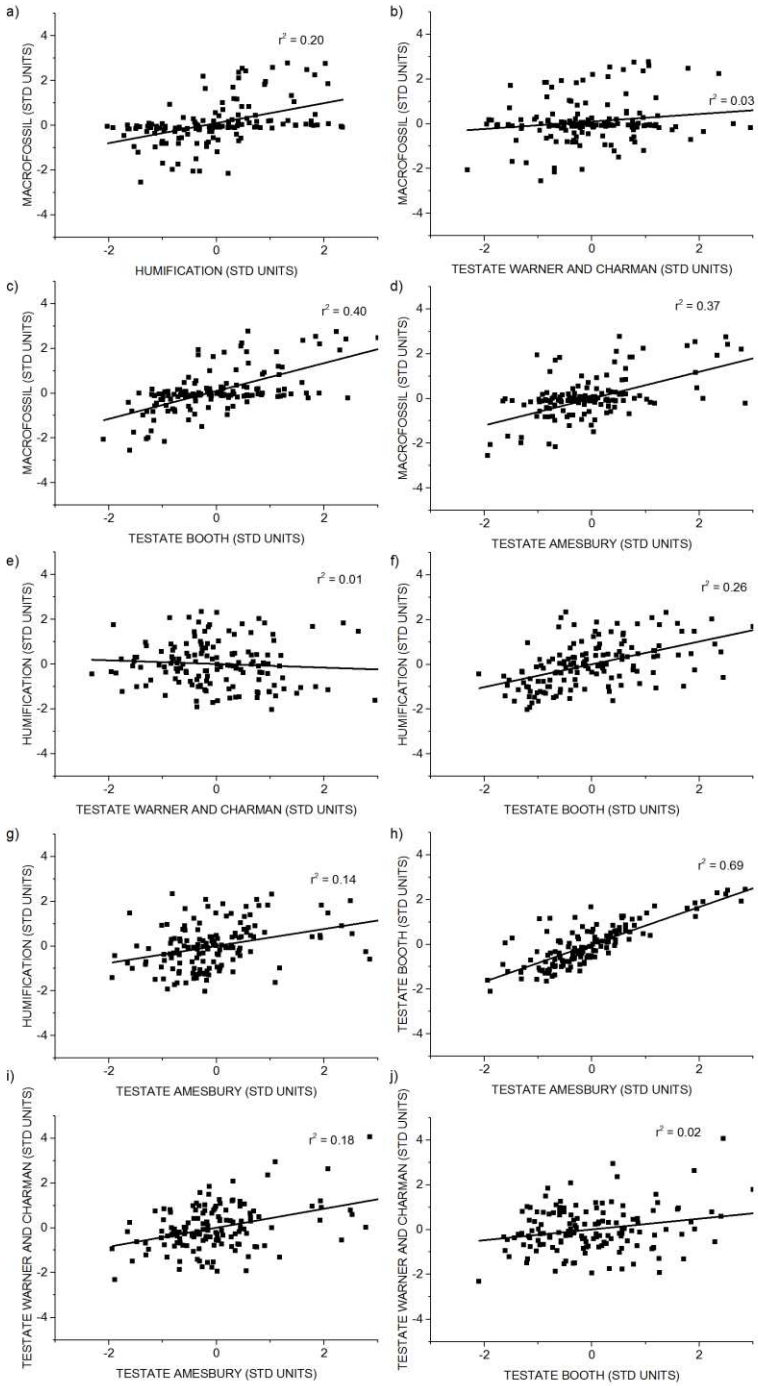

Supplementary Figure 3

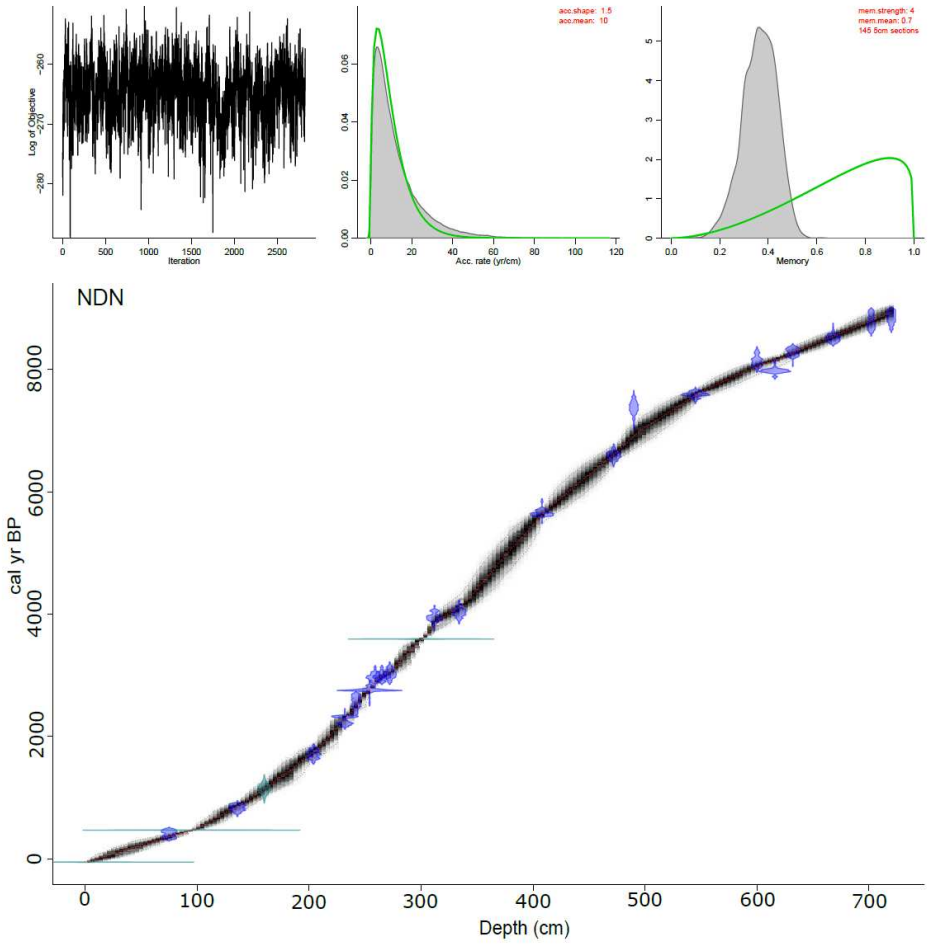

Supplementary Table 1

PNDC			NDN
Macrofossil (HCl)	Humification	Testate amoebae (DTWT)	Testate amoebae (DTWT)
7830 MAR 7626-8014 BP		7830 MAR 7626-8014 BP	**7940 MAR 7800-8053 BP**
7500 MAR 7336 – 7694 BP	7500 MAR 7336 – 7694 BP	7500 MAR 7336 – 7694 BP	**7500 MAR 7330-7627 BP**
7220 MAR 7052-7365 BP	7160 MAR 6951-7318 BP	7220 MAR 7053-7366 BP	**7170 MAR 6930-7378 BP**
6600 MAR 6472-6760 BP	6640 MAR 6517-6797 BP	6600 MAR 6472-6759 BP	**6630 MAR 6504-6772 BP**
6340 MAR 6198-6497 BP	6340 MAR 6198-6497 BP	6340 MAR 6198-6497 BP	**6460 MAR 6236-6641 BP**
6110 MAR 6004-6237 BP	6110 MAR 6004-6237 BP	6110 MAR 6004-6237 BP	**6280 MAR 6031-6505 BP**
	5550 MAR 5389-5655 BP	5550 MAR 5389-5655 BP	5790 MAR 5633-5983 BP
	4750 MAR 4580-4850 BP	5010 MAR 4815-5198 BP	**5180 MAR 4862-5461 BP**
	4440 MAR 4252-4622 BP	4500 MAR 4311 -4669 BP	**4570 MAR 4309-4886 BP**
	4290 MAR 4117-4477 BP	4290 MAR 4117-4477 BP	**4310 MAR 4129-4584 BP**
	3860 MAR 3702 -4011 BP		
	2890 MAR 2646-3131 BP	2950 MAR 2680 -3187 BP	
	2610 MAR 2428-2830 BP	2610 MAR 2428-2830 BP	**2600 MAR 2452-2741 BP**
	2310 MAR 2092-2548 BP	2110 MAR 1974-2319 BP	**2080 MAR 1852-2260 BP**
	1480 MAR 1219-1755 BP	1480 MAR 1219-1755 BP	1780 MAR 1640-1897 BP
	1250 MAR 1060 -1490 BP	1250 MAR 1060 -1490 BP	
	1000 MAR 790-1157 BP		
	290 MAR 161 -467 BP	290 MAR 161 -467 BP	

Supplementary Table 2

	HUMIFICATION	HCI	BOOTH TF	AMESBURY TF
HCI	0.455 (0.000)			
BOOTH TF	0.507 (0.000)	0.633 (0.000)		
AMESBURY TF	0.378 (0.000)	0.610 (0.000)	0.834 (0.000)	
CHARMAN TF	-0.081 (0.321)	0.170 (0.041)	0.240 (0.004)	0.424 (0.000)